Polar Geosci., **19**, 118–151, 2006

Electron microprobe technique for U-Th-Pb and REE chemistry of monazite, and its implications for pre-, peak- and post-metamorphic events of the Lützow-Holm Complex and the Napier Complex, East Antarctica

Tomokazu Hokada[1,2*] and Yoichi Motoyoshi[1,2]

[1] *National Institute of Polar Research, Kaga 1-chome, Itabashi-ku, Tokyo 173-8515*
[2] *Department of Polar Science, School of Multidisciplinary Sciences, The Graduate University for Advanced Studies, Kaga 1-chome, Itabashi-ku, Tokyo 173-8515*
**Corresponding author. E-mail: hokada@nipr.ac.jp*

(Received March 24, 2006; Accepted June 29, 2006)

Abstract: Monazites in high-grade metapelites from the Lützow-Holm Complex and Napier Complex have been examined in terms of U, Th, Pb and rare earth element (REE) chemistry using an electron microprobe. The studied samples include four granulite-facies garnet-biotite-bearing metapelites from Skallen within the Lützow-Holm Complex, and a re-hydrated garnet-sillimanite gneiss from the Mt. Riiser-Larsen area within the UHT zone of the Napier Complex.

Two out of four garnet-bearing metapelitic samples from Skallen gave simple 560–500 Ma monazite U-Th-Pb ages, whereas the other two samples yielded two age populations, *i.e.,* 560–500 Ma and 650–580 Ma. The younger age group is consistent with the 550–520 Ma metamorphic ages reported by SHRIMP. The older >580 Ma monazites are relatively enriched in Nd, Sm, Gd, Dy (MREE) and depleted in Si (Ca and Th) compared with the younger (560–500 Ma) ones. These older monazites possibly formed through M-HREE-enriched conditions such as garnet-free conditions, suggesting that the growth of these monazites pre-dated the peak metamorphism.

Garnet-sillimanite gneiss from the Mt. Riiser-Larsen area shows various post-UHT re-hydration textures such as biotite-sillimanite aggregates, and fine-grained biotite flakes around or intracrystalline fractures within garnet porphyroblasts. Monazites enclosed within garnet cores have 2480–2440 Ma U-Th-Pb ages consistent with the reported zircon and monazite SHRIMP dates. On the other hand, those associated with re-hydrated zones gave fluctuating 2200–700 Ma ages. These younger ages are thought to reflect the incomplete chemical disturbance during the post-UHT crustal processes.

key words: Lützow-Holm Complex, monazite, Napier Complex, rare earth element/REE, U-Th-Pb age

1. Introduction

Electron microprobe (EMP) dating of U-Th-bearing minerals such as monazite, zircon and xenotime, developed from the pioneering work of Suzuki *et al.* (1991) and Suzuki and Adachi (1991), who established the Th-U-total Pb *Ch*emical *I*sochron

*Me*thod (CHIME), has proven to be a powerful tool for estimating geologic ages of igneous and metamorphic rocks, and is now used in laboratories worldwide (*e.g.,* Montel *et al*., 1996; Yokoyama and Saito, 1996; Cocherie *et al*., 1998; Williams *et al*., 1999; Cocherie and Albarede, 2001; Williams and Jercinovic, 2002; Pyle *et al*., 2002, 2005; Jercinovic and Williams, 2005). However, numerous factors (type of spectrometer/detector, detector gas, standard materials/compositions, matrix correction, peak/background positioning, accelerating voltage, correction of peak interferences, etc.) affect U-Th-Pb quantification, and, consequently, age estimates (*e.g.,* Pyle *et al*., 2002, 2005; Jercinovic and Williams, 2005). Differences of analytical protocol between different laboratories makes it difficult to make inter-laboratory comparisons. Apart from age determinations, measurement of rare earth elements (REE) and other elements (P, Si, Ca, U, Th) in monazite is important in understanding accessory phase behavior and geochemistry.

Zhu and O'Nions (1999) suggest that monazite REE chemistry is strongly affected by coexisting phases, especially in the presence of garnet, which controls the heavy rare earth element (HREE) content of monazite. Several studies (*e.g.,* Yokoyama and Saito, 1996; Scherrer *et al*., 2000; Hokada *et al*., 2004) have dealt with full elemental (P+Si+Ca+REE+Y+Th+Pb) chemical analysis for the monazite dating. Such complete analyses are essential to check the reliability of age estimations and to examine consistency with other dating techniques. We have been developing this technique using an electron microprobe (JEOL JXA-8800 with 5ch wavelength dispersive spectrometers) at the National Institute of Polar Research. In this paper, a detailed analytical protocol for U-Th-Pb chemical dating and quantitative REE measurement is described.

The Lützow-Holm Complex and the Napier Complex are high-grade metamorphic terranes located in East Antarctica. These are excellent subjects to examine monazite behavior during high temperature deep crustal processes. U-Pb zircon chronology has been applied to the Lützow-Holm Complex and has demonstrated the age of high-grade metamorphism at 550–520 Ma (Shiraishi *et al*., 1994, 2003). Monazite ages 534±14 Ma and 537±9 Ma obtained by the electron microprobe (EMP) U-Th-Pb chemical isochron method (CHIME) have been reported for two garnet-biotite gneisses from the Lützow-Holm Complex (Asami *et al*., 1997, 2005), and are in the same age brackets with zircon ages. U-Th-Pb and isotopic dating methods, such as Sm-Nd, Rb-Sr and Ar-Ar, have been applied to rocks from the Napier Complex, along with monazite ages, and indicate the occurrence of late Archaean to early Proterozoic (>2590–2450 Ma) UHT and younger Proterozoic (2400–700 Ma) events (Asami *et al*., 1998, 2002; Carson *et al*., 2002; Grew *et al*., 2001; Harley *et al*., 2001; Hokada *et al*., 2004; Kelly and Harley, 2005; Suzuki *et al*., 2006). This paper provides monazite ages combined with chemistry and petrographic context, which make it possible to discuss the pre-, peak- and post-peak metamorphic histories of these terranes.

2. Analytical technique

2.1. Electron microprobe analytical settings

Monazite grains were analyzed in polished thin sections using a JEOL JXA-8800M

Table 1. Electron microprobe analytical settings for monazite. See text for detail.

No.	Element	X-ray	Channel	Crystal	Detector gas	Time (s)	Peak (mm)	BG- (mm)	BG+ (mm)	Base L. (V)	Window (V)	Interference correction
1	P	Kα	2	PET	Xe (sealed)	10	196.76	-7.4	+3.5			
2	Si	Kα	2	PET	Xe (sealed)	10	227.76	-4.7	+3.4			
3	Ca	Kα	2	PET	Xe (sealed)	10	107.37	-4.0	+4.0			
4	Y	Lα	2	PET	Xe (sealed)	10	206.15	-3.8	+1.5			
5	La	Lα	4	LIF	Xe (sealed)	10	185.33	-4.5	+2.7			
6	Ce	Lα	4	LIF	Xe (sealed)	10	178.10	-3.5	+2.8			
7	Pr	Lβ	4	LIF	Xe (sealed)	10	157.05	-1.3	+4.8			
8	Nd	Lβ	4	LIF	Xe (sealed)	10	150.66	-6.2	+5.1			
9	Sm	Lβ	4	LIF	Xe (sealed)	10	138.93	-3.7	+5.6			
10	Gd	Lβ	4	LIF	Xe (sealed)	10	128.38	-1.3	+6.7			
11	Dy	Lα	4	LIF	Xe (sealed)	10	132.70	-5.6	+2.4			
12	Er	Lα	4	LIF	Xe (sealed)	10	124.06	-1.4	+3.2			
13	Yb	Lα	4	LIF	Xe (sealed)	10	116.22	-4.4	+1.7			
14	U	Mβ	1	PET	Ar (flow)	240	118.95	-3.8	+1.4	2.5	3	from Th
15	Th	Mα	2	PET	Xe (sealed)	120	132.21	-3.6	+3.6	2.5	3	
16	Pb	Mβ	3	PETH	Xe (sealed)	240	162.38	-2.6	+3.0	2	3.5	from U

electron microprobe (EMP) with a 5ch wavelength-dispersive X-ray analytical system (WDS) at the National Institute of Polar Research. Analytical conditions were maintained at 15 kV accelerating voltage, 200 nA probe current, and 2 μm probe diameter (with an estimated area of analysis of $<6\mu$m). Natural and synthesized minerals and oxides were used as calibration standards. Prz (modified ZAF) correction (and occasionally ZAF correction) was applied to analyses. Sixteen elements (P, Si, Ca, Y, La, Ce, Pr, Nd, Sm, Gd, Dy, Er, Yb, U, Th and Pb) were analyzed with 3 PET and 1 LIF crystals. Elements and X-ray spectral settings are listed in Table 1. The choices of X-ray peak and background position are based on full WDS scan of natural monazites and interference-free standard materials. Some of the X-ray peaks were measured using a β line to avoid or minimize the element interferences. The position of the U Mβ peak is near the absorption edge of the Ar detector gas; it is essential for the high-background position to be less than 2 mm from the peak position. The spectral interferences of Th on the U Mβ line and U on the Pb Mβ line were corrected on the basis of ratios measured on overlap-free X-ray peaks in standard materials. Recent and detailed discussion of analytical techniques for EMP monazite dating can also be seen in Pyle *et al.* (2002, 2005), Jercinovic and Williams (2005), Suzuki (2005), and references therein.

2.2. Age calculation and evaluation of uncertainty

The theoretical basis of EMP chemical dating essentially follows the Th-U-total Pb isochron method (CHIME) described in Suzuki *et al.* (1991) and Suzuki and Adachi (1991). Suzuki and Adachi (1991) obtained an age from linear regression on a PbO-ThO_2* (=the sum of ThO_2 and the ThO_2 equivalent of UO_2) diagram, assuming that initial PbO is homogeneously distributed in the mineral. The initial Pb (common lead) abundances in monazite are generally small relative to radiogenic Pb (*e.g.*, Jercinovic and Williams, 2005; Pyle *et al.*, 2005), and ages in this study have been

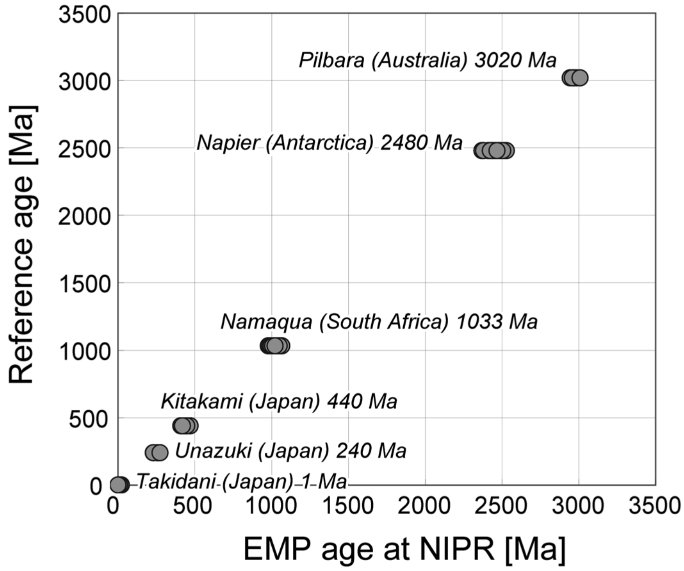

Fig. 1. Comparison of electron microprobe (EMP) chemical ages at NIPR with other reported ages —Pilbara granites: SHRIMP zircon ages by Kiyokawa et al. (2002), Napier granitic gneiss: SHRIMP monazite ages by Suzuki et al. (2006), Namaqualand monazite vein: SHRIMP zircon ages by Knoper et al. (2000), Kitakami and Unazuki granitic rocks: EMP monazite ages by Yokoyama (personal com.), Takidani granites: SHRIMP zircon ages by Sano et al. (2002). Error of each analysis is less than the size of the symbol.

calculated with the assumption that initial PbO is negligible. As chemical analysis using WDS is strongly affected by the choice of the X-ray line for each element, the X-ray matrix correction model (prz or ZAF), background positioning, and choice of standard materials, we have chosen the combination of these factors most suitable for obtaining U-Th-Pb ages consistent with ages reported by SHRIMP U-Pb or other techniques. Figure 1 shows the comparison of several different age determination using our EMP technique with other reported ages. We have calculated the error propagation for each age determination simply from X-ray counting statistics only. As a few percent of shift is inevitable due to the daily drift of machine conditions, we have checked the reproducibility of an age reference monazite (1033 Ma; Knoper *et al.*, 2001) from Namaqualand, South Africa. The drift of the reference age monazite analyses is less than 1% (Fig. 2).

3. Sample description

3.1. Pelitic gneisses from Skallen, Lützow-Holm Complex

The Lützow-Holm Complex (LHC) is an amphibolite to granulite-facies (up to ultrahigh temperature/UHT) metamorphic belt which extends 400 km along the Prince Olav Coast and the eastern coast of Lützow-Holm Bay (Fig. 3). The age of high-grade metamorphism has been well constrained at 550–520 Ma by SHRIMP zircon analysis

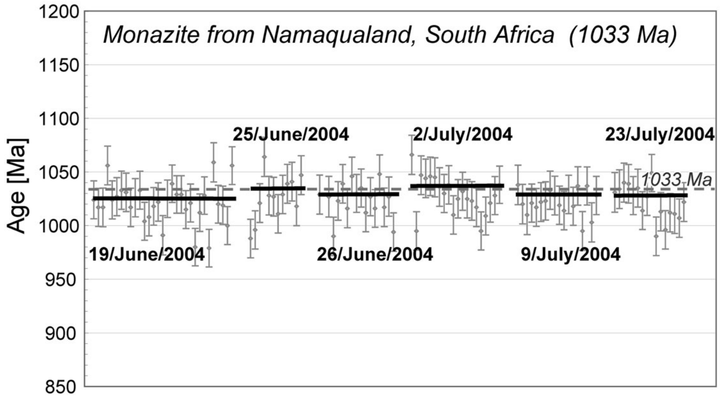

Fig. 2. Drift of EMP ages analyzed for Namaqualand monazite (1033 Ma) at NIPR over a month period (19th/June/2004 to 23rd/July/2004).

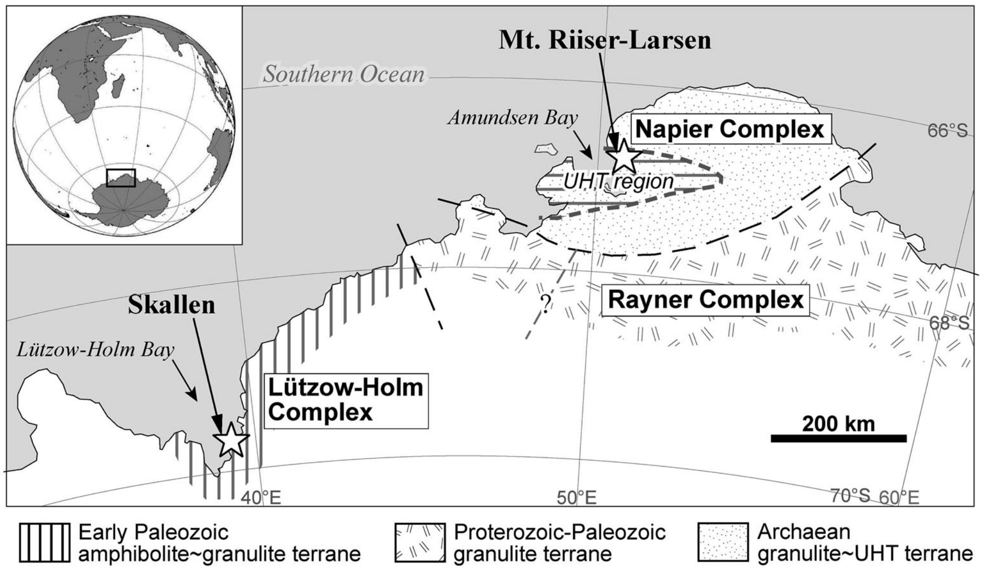

Fig. 3. Geological sketch map of the coastal region of Antarctica from 35–60°E. The locations of EMP dating samples are plotted as open stars.

(Shiraishi *et al*., 1994, 2003). High-grade lithologies have experienced near-isothermal decompression (Hiroi *et al*., 1991; Motoyoshi and Ishikawa, 1997) and subsequent cooling to ~300°C at *c*. 500 Ma (Fraser *et al*., 2000).

Metapelitic samples used in this study were collected at Skallen, which is located within the granulite-facies zone. Skallen is the third largest outcrop along the Sôya Coast, and is underlain by various kinds of high-grade metamorphic rocks and three types of pre- to syn-metamorphic and post-metamorphic intrusive rocks (Osanai *et al*., 2004; Fig. 4). Metamorphic lithologies are subdivided into four main categories:

Table 2. Mineral assemblages of the analyzed samples. Mineral abbreviations are after Kretz (1983).

Sample No.	Abb.	Qtz	Pl	Kfs	Bt	Grt	Sil	Spl	Ap	Zrn	Mnz	Opq	note
Skallen, Lützow-Holm Complex													
A97122303A	2303A	+	+	+	-	+			+	-	-	Ilm	
A97121901A	1901A	+	+	-	-	+			+	-	-	Ilm	
A97121901B	1901B	-	+	+	-	+		+		-	+	Ilm	Spl is not in contact with Qtz
A97121901E	1901E	+	+	-	+	+			-	-	+	Ilm	
Mt. Riiser-Larsen, Napier Complex													
TH97021409	21409	+	+	-	-	+	+	-		-	-	-	

+: present, -: minor

pelitic and quartzo-feldspathic rocks, mafic and intermediate rocks, calc-silicate rocks, and granitic rocks. Five pelitic gneiss samples used in this study (A97121901A, A97121901B, A97121901E and A97122303A, abbreviated as 1901A, 1901B, 1901E and 2303A hereafter; Table 2), with mineral assemblages including garnet, biotite, quartz, plagioclase and alkali feldspar (plus spinel in sp.1901B), occur as thin layers in alternation with quartzo-feldspathic, calc-cilicate and mafic gneisses (Fig. 4). No reaction relations of constituent minerals are observed in these gneisses.

3.2. Pelitic gneiss from Mt. Riiser-Larsen, Napier Complex

The Napier Complex is an Archaean to Early Proterozoic granulite terrane covering a coastal area between 46°–57°E longitude in East Antarctica (Fig. 3). It consists of tonalitic-granodioritic orthogneisses, garnet-bearing peraluminous granitic gneiss and mafic-ultramafic granulites with subordinate amounts of quartzo-feldspathic, siliceous and aluminous paragneisses, metamorphosed at granulite-facies, partly UHT (>900–1100°C), conditions. The earliest recorded event in the complex is *c.* 3800 Ma tonalitic magmatism, followed by multiple igneous (*c.* 3300–2630 Ma) and metamorphic (*c.* 2840 Ma, ~2590–2460 Ma, and younger) events (*e.g.,* Sheraton *et al.*, 1987; Harley and Black, 1997; Carson *et al.*, 2002; Hokada *et al.*, 2003; Kelly and Harley, 2005; Suzuki *et al.*, 2006, and references therein). The timing of the UHT event is still debated as either 2480–2460 Ma or >2590–2550 Ma (Kelly and Harley, 2005, and references therein), but monazite ages typically give 2480 Ma or younger ages (*e.g.,* Hokada *et al.*, 2004; Suzuki *et al.*, 2006). This at least implies that major thermal events (including UHT metamorphism) terminated *c.* 2480 Ma. Post-2480 isotopic ages for the Napier Complex have been reported by several methods (2200 Ma, 1700 Ma and 700 Ma xenotime or monazite ages by Grew *et al.*, 2001; 1557 and 1897 Ma Sm-Nd garnet-whole rock ages by Owada *et al.*, 2001; 2200 Ma Sm-Nd internal isochron age by Suzuki *et al.*, 2001; ~2380 Ma Sm-Nd internal isochron age by Suzuki *et al.*, 2006). One of our aims for monazite dating is to interpret these post-UHT ages.

Metapelitic samples used in this study were collected from the Mt. Riiser-Larsen area, located on the northeast coast of Amundsen Bay in the UHT zone of the Napier Complex (Fig. 5). The study area is mainly composed of orthopyroxene-bearing orthogneiss with tonalitic-granodioritic compositions, garnet-bearing felsic gneiss with granitic compositions and two-pyroxene-bearing mafic granulite (Ishizuka *et al.*, 1998; Ishikawa *et al.*, 2000). Subordinate pelitic, psammitic, siliceous, aluminous and ferru-

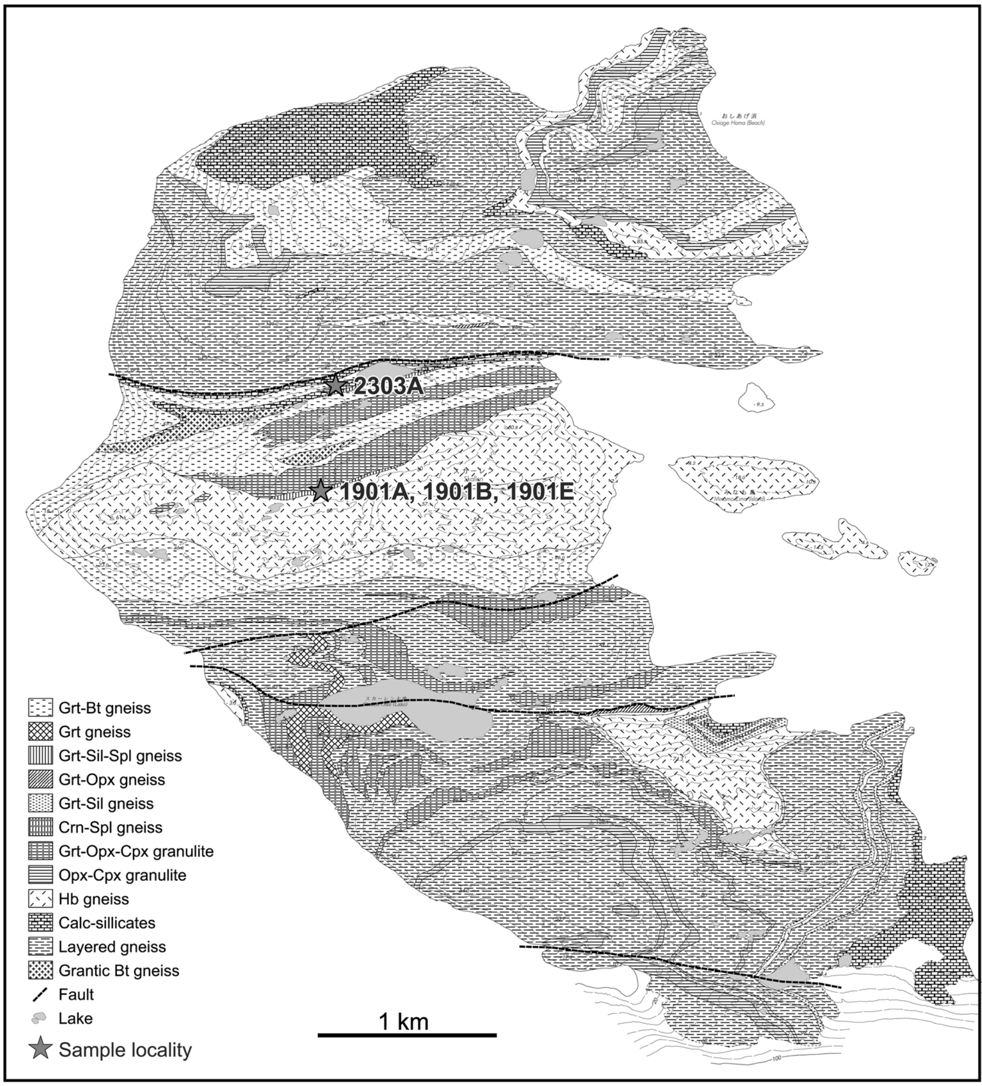

Fig. 4. Geological map of Skallen, Lützow-Holm Complex (Osanai et al., 2004) with EMP sample localities.

ginous paragneisses, pyroxenite and ultramafic granulite are also present. These gneisses contain almost totally anhydrous mineral assemblages consistent with the UHT metamorphic conditions, and secondary hydrous minerals, mostly biotite, are occasionally formed. The analyzed metapelitic sample (sp. TH97021409, denoted as 21409 hereafter) was collected from an outcrop of layered gneiss. It is composed of quartz, plagioclase, garnet, sillimanite with minor biotite, monazite and opaque minerals. Quartz and plagioclase form granoblastic grains 0.2–2 mm in diameter. Garnet is porphyroblastic and occasionally up to 1 cm in diameter. Prismatic sillimanite 1–2 mm in length is occasionally aligned to form a foliation. Fine-grained (<0.1 mm) biotite

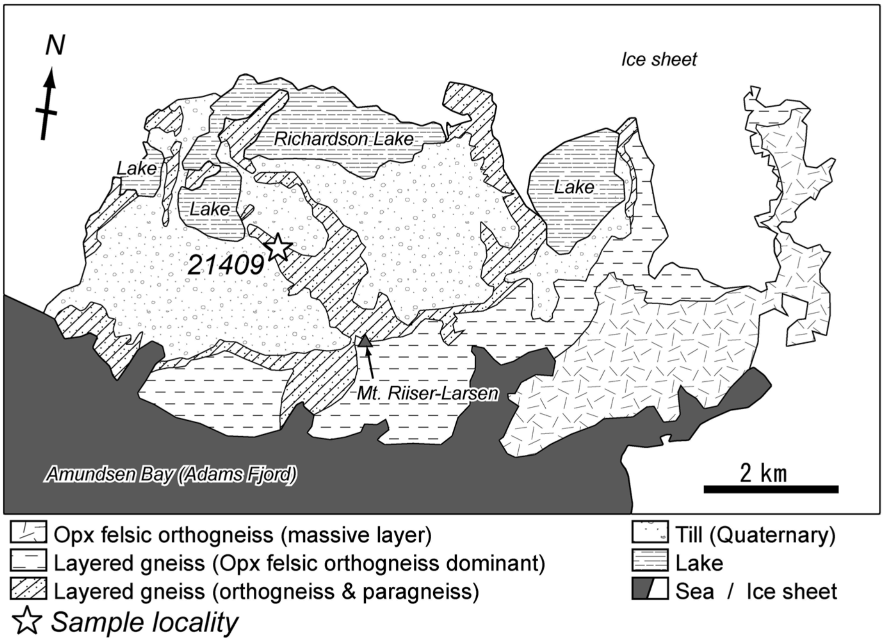

Fig. 5. Geological map of Mt. Riiser-Larsen, Napier Complex (simplified after Ishikawa et al., 2000) with EMP sample locality.

occurs commonly around and in fractures within garnet, or as fine-grained aggregates with sillimanite.

4. Results of EMP analyses

4.1. Monazite chemical data

Representative electron microprobe data of monazites from Skallen and the Mt. Riiser-Larsen area are listed in Tables 3 and 4, and summarized in Table 5. For Skallen samples, averaged compositions (with standard deviations) are presented in Table 3 for each domain/grain, from a total of 566 analytical spots on 157 monazite grains. For the Mt. Riiser-Larsen sample, all analytical data (38 analytical spots on 13 monazite grains) are listed in Table 4. Monazite favors light rare earth elements (LREE) over heavy rare earth elements (HREE), and Nd/La and Gd/Nd ratios are typically 0.3–0.5 and $<$ 0.3, respectively. Apparent U-Th-Pb chemical ages have been calculated on the basis of measured U:Th:Pb ratios. Age errors given in Tables 3, 4 and 5, and Fig. 6, are at 1-sigma (67.8% confidence level) and derived from X-ray counting statistics only. Errors calculated for weighted average ages using the computer program ISOPLOT provided by K.R. Ludwig at Barkley Geochemistry Center of University of California (Ludwig, 2001) are at 2-sigma (95% confidence level).

4.2. Monazite ages and chemistry from the Lützow-Holm samples

Most U-Th-Pb chemical ages range from 660 Ma to 500 Ma. Two samples (2303A

Table 3. Representative chemical compositions of monazites in pelitic gneisses from Skallen, Lützow-Holm Complex, East Antarctica.

Sample		SK2303A		SK2303A		SK2303A		SK2303A		SK2303A		SK2303A		SK1901A		SK1901A	
Grain #		mnz-#1		mnz-#1		mnz-#1		mnz-#1		mnz-#1		mnz-#1		mnz-#2		mnz-#3	
spot		zone-I		zone-II		zone-III		zone-IV		zone-V		zone-VI					
	detection limit	*average*	*s.d.*	*average*	*s.d.*	*average*	*s.d.*	*average*	*s.d.*	*average*	*s.d.*	*average*	*s.d.*	*average*	*s.d.*	*average*	*s.d.*
wt%		*n=4*		*n=4*		*n=4*		*n=4*		*n=6*		*n=4*		*n=11*		*n=11*	
P_2O_5		27.23	*0.32*	27.45	*0.40*	27.40	*0.31*	26.01	*0.36*	24.70	*0.54*	22.50	*0.29*	29.13	*0.64*	29.41	*1.44*
SiO_2		1.80	*0.06*	1.52	*0.07*	1.33	*0.05*	1.56	*0.04*	2.43	*0.28*	3.61	*0.21*	2.19	*0.39*	2.40	*0.72*
CaO		0.74	*0.01*	0.69	*0.01*	0.63	*0.02*	0.70	*0.02*	0.77	*0.04*	0.87	*0.01*	0.84	*0.07*	0.86	*0.10*
Y_2O_3	*0.03*	0.03	*0.03*	d.l.		0.05	*0.03*	d.l.		d.l.		d.l.		d.l.		d.l.	
La_2O_3	*0.05*	16.82	*0.10*	17.28	*0.20*	16.87	*0.39*	17.13	*0.08*	16.02	*0.49*	14.18	*0.20*	17.10	*0.51*	16.89	*0.64*
Ce_2O_3	*0.04*	29.80	*0.27*	30.38	*0.31*	30.77	*0.34*	29.71	*0.37*	28.48	*0.89*	25.15	*0.17*	29.35	*0.69*	28.86	*1.27*
Pr_2O_3	*0.09*	3.30	*0.14*	3.33	*0.12*	3.45	*0.15*	3.19	*0.15*	3.10	*0.15*	2.80	*0.16*	3.12	*0.10*	3.10	*0.15*
Nd_2O_3	*0.07*	9.53	*0.07*	9.53	*0.09*	9.90	*0.22*	9.48	*0.14*	8.93	*0.13*	8.51	*0.06*	9.02	*0.26*	9.03	*0.46*
Sm_2O_3	*0.07*	0.87	*0.07*	0.93	*0.08*	1.01	*0.02*	0.98	*0.07*	0.77	*0.05*	0.85	*0.11*	0.63	*0.10*	0.63	*0.10*
Gd_2O_3	*0.07*	0.29	*0.12*	0.34	*0.10*	0.34	*0.07*	0.35	*0.11*	0.27	*0.16*	0.32	*0.11*	0.18	*0.09*	0.09	*0.10*
Dy_2O_3	*0.04*	d.l.		d.l.		0.04	*0.03*	d.l.		d.l.		d.l.		d.l.		d.l.	
Er_2O_3	*0.04*	d.l.		d.l.		d.l.		d.l.		d.l.		d.l.		d.l.		d.l.	
Yb_2O_3	*0.05*	d.l.		d.l.		d.l.		d.l.		d.l.		d.l.		d.l.		d.l.	
UO_2	*0.007*	0.092	*0.006*	0.092	*0.005*	0.106	*0.010*	0.097	*0.012*	0.116	*0.017*	0.149	*0.006*	0.155	*0.019*	0.175	*0.043*
ThO_2	*0.006*	9.865	*0.136*	8.700	*0.227*	7.878	*0.137*	9.250	*0.287*	13.248	*1.241*	19.450	*0.755*	11.703	*1.500*	12.594	*2.624*
PbO	*0.004*	0.237	*0.009*	0.212	*0.008*	0.184	*0.007*	0.224	*0.004*	0.316	*0.030*	0.463	*0.019*	0.279	*0.039*	0.299	*0.067*
Total		100.89	*0.45*	100.72	*0.76*	100.21	*0.43*	99.05	*0.41*	99.49	*0.52*	99.09	*0.74*	103.99	*0.42*	104.63	*0.62*
Cations (O=4)																	
P		0.922	*0.004*	0.930	*0.006*	0.934	*0.005*	0.910	*0.005*	0.872	*0.012*	0.816	*0.009*	0.938	*0.015*	0.938	*0.030*
Si		0.072	*0.002*	0.061	*0.003*	0.053	*0.002*	0.065	*0.002*	0.101	*0.012*	0.155	*0.008*	0.083	*0.015*	0.091	*0.029*
Ca		0.032	*0.001*	0.030	*0.000*	0.027	*0.001*	0.031	*0.001*	0.034	*0.002*	0.040	*0.001*	0.034	*0.003*	0.035	*0.004*
Y		0.001	*0.001*	-	-	0.001	*0.001*	-	-	-	-	-	-	-	-	-	-
La		0.248	*0.002*	0.255	*0.004*	0.250	*0.005*	0.261	*0.002*	0.246	*0.007*	0.224	*0.004*	0.240	*0.007*	0.235	*0.005*
Ce		0.436	*0.004*	0.445	*0.004*	0.453	*0.005*	0.449	*0.004*	0.435	*0.013*	0.395	*0.005*	0.409	*0.008*	0.398	*0.011*
Pr		0.048	*0.002*	0.049	*0.002*	0.051	*0.002*	0.048	*0.002*	0.047	*0.002*	0.044	*0.002*	0.043	*0.001*	0.043	*0.001*
Nd		0.136	*0.001*	0.136	*0.002*	0.142	*0.004*	0.140	*0.002*	0.133	*0.003*	0.130	*0.001*	0.122	*0.003*	0.121	*0.004*
Sm		0.012	*0.001*	0.013	*0.001*	0.014	*0.000*	0.014	*0.001*	0.011	*0.001*	0.013	*0.002*	0.008	*0.001*	0.008	*0.001*
Gd		0.004	*0.002*	0.004	*0.001*	0.005	*0.001*	0.005	*0.001*	0.004	*0.002*	0.005	*0.001*	0.002	*0.001*	0.001	*0.001*
Dy		-	-	-	-	0.000	*0.000*	-	-	-	-	-	-	-	-	-	-
Er		-	-	-	-	-	-	-	-	-	-	-	-	-	-	-	-
Yb		-	-	-	-	-	-	-	-	-	-	-	-	-	-	-	-
U		0.001	*0.000*	0.001	*0.000*	0.001	*0.000*	0.001	*0.000*	0.001	*0.000*	0.001	*0.000*	0.001	*0.000*	0.001	*0.000*
Th		0.090	*0.001*	0.079	*0.002*	0.072	*0.001*	0.087	*0.003*	0.126	*0.012*	0.190	*0.007*	0.101	*0.013*	0.108	*0.024*
Pb		0.003	*0.000*	0.002	*0.000*	0.002	*0.000*	0.002	*0.000*	0.004	*0.000*	0.005	*0.000*	0.003	*0.000*	0.003	*0.001*
Total		2.009	*0.003*	2.009	*0.003*	2.011	*0.004*	2.019	*0.002*	2.021	*0.004*	2.021	*0.003*	1.991	*0.002*	1.986	*0.003*
Nd/La		0.295	*0.003*	0.288	*0.003*	0.306	*0.014*	0.289	*0.005*	0.291	*0.012*	0.313	*0.004*	0.275	*0.006*	0.279	*0.007*
Gd/Nd		0.072	*0.029*	0.082	*0.025*	0.080	*0.014*	0.086	*0.026*	0.071	*0.042*	0.088	*0.029*	0.047	*0.024*	0.023	*0.025*
UO_2*		3.19	*0.05*	2.82	*0.07*	2.58	*0.05*	3.00	*0.10*	4.28	*0.40*	6.26	*0.23*	3.83	*0.49*	4.13	*0.86*
ThO_2*		10.17	*0.15*	9.01	*0.22*	8.23	*0.15*	9.57	*0.30*	13.63	*1.26*	19.94	*0.74*	12.22	*1.55*	13.17	*2.76*
Th/U		110.19	*5.95*	96.62	*6.92*	76.20	*6.95*	98.94	*11.43*	119.12	*20.34*	134.09	*10.68*	77.34	*6.02*	74.44	*5.69*
Age [Ma]		550	*24*	554	*21*	528	*12*	553	*13*	548	*9*	547	*3*	538	*20*	534	*11*
+/- [Ma]		18	*0*	20	*0*	22	*0*	19	*1*	13	*1*	9	*0*	15	*2*	14	*3*

d.l.: below detection limit

Table 3 (continued).

Sample	SK1901A		SK1901A		SK1901A		SK1901A		SK1901A		SK1901B		SK1901B		SK1901B		SK1901B	
Grain #	mnz-#4		mnz-#5		mnz-#6		mnz-#8		mnz-#9		m-1		m-2		m-3		m-4	
spot															(in grt)		(in grt)	
	average	*s.d.*	*average*	*s.d.*	*average*	*s.d.*	*average*	*s.d.*	*average*	*s.d.*	*average*	*s.d.*	*average*	*s.d.*	*average*	*s.d.*	*average*	*s.d.*
Wt%	*n=16*		*n=9*		*n=7*		*n=9*		*n=9*		*n=15*		*n=16*		*n=8*		*n=10*	
P_2O_5	32.02	*0.67*	29.64	*0.71*	31.85	*0.63*	32.30	*0.36*	32.63	*0.48*	27.36	*0.25*	27.95	*0.53*	27.48	*0.59*	27.40	*0.44*
SiO_2	0.74	*0.33*	2.15	*0.33*	0.91	*0.36*	0.61	*0.15*	0.61	*0.24*	0.43	*0.11*	0.27	*0.16*	0.34	*0.21*	0.49	*0.14*
CaO	0.57	*0.21*	0.84	*0.09*	0.66	*0.15*	0.59	*0.12*	0.52	*0.16*	1.67	*0.16*	1.03	*0.37*	1.34	*0.41*	1.58	*0.25*
Y_2O_3	d.l.		d.l.		d.l.		d.l.		d.l.		0.21	*0.12*	0.82	*0.55*	0.48	*0.24*	0.26	*0.34*
La_2O_3	19.11	*0.90*	16.75	*0.42*	18.67	*0.51*	19.05	*0.30*	19.05	*0.56*	14.69	*0.47*	15.94	*0.68*	15.21	*0.81*	15.11	*0.65*
Ce_2O_3	32.89	*1.33*	29.67	*0.78*	32.19	*1.07*	32.61	*0.71*	32.74	*0.82*	29.07	*0.60*	29.82	*0.65*	29.81	*0.92*	29.17	*0.38*
Pr_2O_3	3.49	*0.19*	3.17	*0.07*	3.42	*0.18*	3.46	*0.12*	3.52	*0.13*	3.53	*0.07*	3.62	*0.13*	3.58	*0.07*	3.48	*0.10*
Nd_2O_3	10.07	*0.36*	9.21	*0.18*	10.03	*0.42*	10.31	*0.30*	10.27	*0.42*	11.07	*0.21*	11.30	*0.28*	11.32	*0.27*	10.79	*0.23*
Sm_2O_3	0.72	*0.09*	0.60	*0.07*	0.75	*0.13*	0.78	*0.07*	0.79	*0.11*	1.59	*0.14*	1.77	*0.25*	1.73	*0.23*	1.50	*0.22*
Gd_2O_3	0.14	*0.09*	0.12	*0.10*	0.16	*0.09*	0.19	*0.09*	0.19	*0.15*	0.72	*0.18*	1.03	*0.36*	0.91	*0.30*	0.65	*0.26*
Dy_2O_3	d.l.		d.l.		d.l.		d.l.		d.l.		0.09	*0.06*	0.32	*0.18*	0.19	*0.11*	0.13	*0.14*
Er_2O_3	d.l.		d.l.		d.l.		d.l.		d.l.		d.l.		0.05	*0.05*	d.l.		d.l.	
Yb_2O_3	d.l.		d.l.		d.l.		d.l.		d.l.		d.l.		d.l.		d.l.		d.l.	
UO_2	0.100	*0.012*	0.115	*0.027*	0.101	*0.007*	0.102	*0.006*	0.103	*0.011*	0.860	*0.351*	0.728	*0.303*	0.427	*0.197*	0.576	*0.308*
ThO_2	4.749	*2.248*	11.520	*1.484*	5.780	*2.021*	4.369	*1.081*	4.089	*1.771*	7.274	*0.763*	4.226	*2.289*	6.050	*2.428*	7.380	*1.518*
PbO	0.114	*0.049*	0.280	*0.035*	0.139	*0.048*	0.109	*0.022*	0.101	*0.038*	0.244	*0.037*	0.168	*0.036*	0.187	*0.050*	0.228	*0.024*
Total	104.98	*0.71*	104.38	*0.43*	104.93	*0.44*	104.79	*0.37*	104.94	*0.38*	99.14	*0.49*	99.53	*0.70*	99.59	*0.42*	99.14	*0.54*
Cations (O=4)																		
P	0.998	*0.012*	0.946	*0.015*	0.993	*0.013*	1.005	*0.007*	1.009	*0.010*	0.946	*0.005*	0.957	*0.009*	0.947	*0.012*	0.947	*0.008*
Si	0.027	*0.012*	0.081	*0.013*	0.034	*0.013*	0.022	*0.006*	0.022	*0.009*	0.018	*0.004*	0.011	*0.006*	0.014	*0.009*	0.020	*0.006*
Ca	0.023	*0.008*	0.034	*0.003*	0.026	*0.006*	0.023	*0.005*	0.020	*0.007*	0.073	*0.007*	0.045	*0.016*	0.059	*0.018*	0.069	*0.011*
Y	-	-	-	-	-	-	-	-	-	-	0.005	*0.003*	0.018	*0.012*	0.010	*0.005*	0.006	*0.007*
La	0.259	*0.010*	0.233	*0.005*	0.254	*0.005*	0.258	*0.004*	0.257	*0.007*	0.221	*0.007*	0.238	*0.009*	0.228	*0.011*	0.227	*0.009*
Ce	0.443	*0.014*	0.409	*0.009*	0.434	*0.013*	0.439	*0.009*	0.438	*0.011*	0.435	*0.009*	0.442	*0.008*	0.444	*0.012*	0.436	*0.004*
Pr	0.047	*0.002*	0.044	*0.001*	0.046	*0.002*	0.046	*0.002*	0.047	*0.002*	0.052	*0.001*	0.053	*0.002*	0.053	*0.001*	0.052	*0.002*
Nd	0.132	*0.004*	0.124	*0.002*	0.132	*0.005*	0.135	*0.004*	0.134	*0.005*	0.162	*0.003*	0.163	*0.003*	0.165	*0.003*	0.157	*0.004*
Sm	0.009	*0.001*	0.008	*0.001*	0.009	*0.002*	0.010	*0.001*	0.010	*0.001*	0.022	*0.002*	0.025	*0.003*	0.024	*0.003*	0.021	*0.003*
Gd	0.002	*0.001*	0.002	*0.001*	0.002	*0.001*	0.002	*0.001*	0.002	*0.002*	0.010	*0.002*	0.014	*0.005*	0.012	*0.004*	0.009	*0.004*
Dy	-	-	-	-	-	-	-	-	-	-	0.001	*0.001*	0.004	*0.002*	0.003	*0.002*	0.002	*0.002*
Er	-	-	-	-	-	-	-	-	-	-	-	-	0.001	*0.001*	-	-	-	-
Yb	-	-	-	-	-	-	-	-	-	-	-	-	-	-	-	-	-	-
U	0.001	*0.000*	0.001	*0.000*	0.001	*0.000*	0.001	*0.000*	0.001	*0.000*	0.008	*0.003*	0.007	*0.003*	0.004	*0.002*	0.005	*0.003*
Th	0.040	*0.019*	0.099	*0.013*	0.049	*0.017*	0.037	*0.009*	0.034	*0.015*	0.068	*0.007*	0.039	*0.021*	0.056	*0.023*	0.069	*0.014*
Pb	0.001	*0.000*	0.003	*0.000*	0.001	*0.000*	0.001	*0.000*	0.001	*0.000*	0.003	*0.000*	0.002	*0.000*	0.002	*0.001*	0.003	*0.000*
Total	1.986	*0.002*	1.987	*0.003*	1.985	*0.002*	1.984	*0.003*	1.981	*0.003*	2.029	*0.003*	2.024	*0.004*	2.029	*0.004*	2.027	*0.003*
Nd/La	0.275	*0.009*	0.287	*0.006*	0.280	*0.008*	0.282	*0.007*	0.281	*0.009*	0.394	*0.017*	0.370	*0.012*	0.389	*0.017*	0.373	*0.021*
Gd/Nd	0.033	*0.022*	0.031	*0.025*	0.037	*0.021*	0.043	*0.022*	0.043	*0.036*	0.152	*0.039*	0.211	*0.073*	0.186	*0.060*	0.140	*0.057*
ThO_2*	5.08	*2.28*	11.90	*1.55*	6.12	*2.03*	4.71	*1.08*	4.43	*1.80*	10.13	*1.06*	6.65	*1.69*	7.47	*2.47*	9.30	*1.06*
Th/U	47.19	*19.48*	105.54	*17.11*	58.09	*18.86*	44.04	*11.46*	39.72	*13.02*	10.51	*5.27*	8.42	*7.23*	16.56	*8.57*	18.11	*11.39*
Age [Ma]	546	*61*	555	*10*	533	*30*	551	*22*	545	*30*	565	*31*	600	*43*	600	*40*	581	*38*
+/- [Ma]	52	*44*	15	*2*	33	*10*	41	*11*	47	*17*	19	*2*	31	*9*	27	*6*	20	*3*

Table 3 (continued).

Sample	SK1901B		SK1901B		SK1901B		SK1901B		SK1901B		SK1901B		SK1901B		SK1901B		SK1901B	
Grain #	m-5		m-6		m-7		m-8		m-9		m-102		m-103		m-104		m-105	
spot	(in grt)				(with zrn)				(in grt)									
	average	*s.d.*	*average*	*s.d.*	*average*	*s.d.*	*average*	*s.d.*	*average*	*s.d.*	*average*	*s.d.*	*average*	*s.d.*	*average*	*s.d.*	*average*	*s.d.*
Wt%	*n=7*		*n=22*		*n=4*		*n=12*		*n=4*		*n=5*		*n=13*		*n=8*		*n=7*	
P_2O_5	27.47	*0.34*	27.38	*0.28*	27.63	*0.17*	27.37	*0.30*	27.86	*0.35*	26.92	*0.35*	27.21	*0.35*	27.15	*0.42*	27.98	*0.38*
SiO_2	0.35	*0.12*	0.37	*0.06*	0.45	*0.04*	0.79	*0.10*	0.40	*0.04*	0.51	*0.05*	0.39	*0.14*	0.43	*0.14*	0.42	*0.21*
CaO	1.04	*0.31*	1.42	*0.11*	1.02	*0.07*	1.51	*0.09*	0.87	*0.06*	1.52	*0.12*	1.36	*0.15*	1.27	*0.16*	1.14	*0.54*
Y_2O_3	0.31	*0.24*	0.21	*0.04*	0.54	*0.05*	0.10	*0.03*	0.19	*0.04*	0.27	*0.18*	0.24	*0.23*	0.21	*0.14*	0.34	*0.32*
La_2O_3	16.19	*0.44*	15.46	*0.25*	16.26	*0.16*	15.47	*0.38*	16.83	*0.17*	14.69	*0.38*	15.33	*0.28*	15.59	*0.32*	16.03	*0.87*
Ce_2O_3	30.55	*1.01*	29.54	*0.34*	30.58	*0.30*	29.53	*0.36*	30.98	*0.32*	29.04	*0.40*	29.90	*0.47*	30.01	*0.45*	30.32	*0.87*
Pr_2O_3	3.65	*0.26*	3.61	*0.10*	3.54	*0.09*	3.46	*0.12*	3.66	*0.10*	3.65	*0.07*	3.64	*0.13*	3.59	*0.09*	3.68	*0.14*
Nd_2O_3	11.14	*0.86*	11.09	*0.13*	11.04	*0.03*	10.45	*0.16*	11.02	*0.18*	11.24	*0.17*	11.22	*0.28*	11.15	*0.21*	11.22	*0.49*
Sm_2O_3	1.64	*0.28*	1.70	*0.11*	1.64	*0.11*	1.17	*0.12*	1.61	*0.04*	1.52	*0.06*	1.56	*0.20*	1.61	*0.14*	1.63	*0.26*
Gd_2O_3	0.78	*0.13*	0.84	*0.10*	0.87	*0.06*	0.42	*0.11*	0.77	*0.16*	0.61	*0.13*	0.77	*0.25*	0.84	*0.18*	0.75	*0.35*
Dy_2O_3	0.11	*0.10*	0.10	*0.04*	0.21	*0.02*	d.l.		0.12	*0.04*	0.08	*0.07*	0.11	*0.10*	0.09	*0.08*	0.14	*0.13*
Er_2O_3	d.l.		d.l.		d.l.		d.l.		d.l.		d.l.		d.l.		0.04	*0.03*	d.l.	
Yb_2O_3	d.l.		d.l.		0.04	*0.03*	d.l.		d.l.		d.l.		d.l.		d.l.		d.l.	
UO_2	0.622	*0.234*	0.804	*0.093*	0.745	*0.013*	0.234	*0.081*	0.311	*0.028*	0.634	*0.159*	0.478	*0.117*	0.634	*0.121*	0.703	*0.299*
ThO_2	4.679	*1.680*	6.121	*0.561*	4.780	*0.227*	8.784	*0.777*	4.570	*0.420*	7.390	*0.689*	6.240	*1.003*	5.868	*1.200*	5.193	*3.169*
PbO	0.164	*0.052*	0.223	*0.015*	0.198	*0.010*	0.219	*0.017*	0.148	*0.006*	0.221	*0.018*	0.189	*0.022*	0.193	*0.018*	0.174	*0.051*
Total	99.04	*0.62*	99.20	*0.44*	100.00	*0.23*	99.85	*0.45*	99.76	*0.25*	98.53	*0.29*	98.99	*0.38*	99.00	*0.47*	100.06	*0.43*
Cations (O=4)																		
P	0.950	*0.006*	0.947	*0.005*	0.947	*0.004*	0.939	*0.005*	0.954	*0.006*	0.940	*0.006*	0.945	*0.007*	0.944	*0.009*	0.954	*0.010*
Si	0.014	*0.005*	0.015	*0.002*	0.018	*0.002*	0.032	*0.004*	0.016	*0.002*	0.021	*0.002*	0.016	*0.006*	0.018	*0.006*	0.017	*0.009*
Ca	0.046	*0.013*	0.062	*0.005*	0.044	*0.003*	0.066	*0.004*	0.038	*0.003*	0.067	*0.006*	0.060	*0.007*	0.056	*0.007*	0.049	*0.023*
Y	0.007	*0.005*	0.005	*0.001*	0.012	*0.001*	0.002	*0.001*	0.004	*0.001*	0.006	*0.004*	0.005	*0.005*	0.005	*0.003*	0.007	*0.007*
La	0.244	*0.008*	0.233	*0.004*	0.243	*0.003*	0.231	*0.006*	0.251	*0.003*	0.224	*0.006*	0.232	*0.004*	0.236	*0.004*	0.238	*0.012*
Ce	0.457	*0.015*	0.442	*0.004*	0.453	*0.005*	0.438	*0.005*	0.459	*0.003*	0.439	*0.007*	0.449	*0.007*	0.451	*0.007*	0.447	*0.012*
Pr	0.054	*0.004*	0.054	*0.002*	0.052	*0.001*	0.051	*0.002*	0.054	*0.001*	0.055	*0.001*	0.054	*0.002*	0.054	*0.001*	0.054	*0.002*
Nd	0.163	*0.012*	0.162	*0.002*	0.160	*0.000*	0.151	*0.002*	0.159	*0.002*	0.166	*0.003*	0.164	*0.003*	0.163	*0.003*	0.161	*0.007*
Sm	0.023	*0.004*	0.024	*0.001*	0.023	*0.002*	0.016	*0.002*	0.022	*0.000*	0.022	*0.001*	0.022	*0.003*	0.023	*0.002*	0.023	*0.004*
Gd	0.011	*0.002*	0.011	*0.001*	0.012	*0.001*	0.006	*0.002*	0.010	*0.002*	0.008	*0.002*	0.010	*0.003*	0.011	*0.002*	0.010	*0.005*
Dy	0.001	*0.001*	0.001	*0.001*	0.003	*0.000*	-	-	0.002	*0.000*	0.001	*0.001*	0.001	*0.001*	0.001	*0.001*	0.002	*0.002*
Er	-	-	-	-	-	-	-	-	-	-	-	-	-	-	0.000	*0.000*	-	-
Yb	-	-	-	-	0.000	*0.000*	-	-	-	-	-	-	-	-	-	-	-	-
U	0.006	*0.002*	0.007	*0.001*	0.007	*0.000*	0.002	*0.001*	0.003	*0.000*	0.006	*0.001*	0.004	*0.001*	0.006	*0.001*	0.006	*0.003*
Th	0.043	*0.015*	0.057	*0.005*	0.044	*0.002*	0.081	*0.007*	0.042	*0.004*	0.069	*0.007*	0.058	*0.010*	0.055	*0.011*	0.048	*0.029*
Pb	0.002	*0.001*	0.002	*0.000*	0.002	*0.000*	0.002	*0.000*	0.002	*0.000*	0.002	*0.000*	0.002	*0.000*	0.002	*0.000*	0.002	*0.001*
Total	2.027	*0.003*	2.029	*0.003*	2.027	*0.003*	2.024	*0.002*	2.022	*0.003*	2.030	*0.003*	2.030	*0.003*	2.030	*0.003*	2.023	*0.003*
Nd/La	0.359	*0.031*	0.374	*0.007*	0.354	*0.004*	0.352	*0.010*	0.341	*0.005*	0.399	*0.016*	0.382	*0.010*	0.373	*0.006*	0.365	*0.009*
Gd/Nd	0.165	*0.035*	0.175	*0.022*	0.184	*0.012*	0.095	*0.025*	0.163	*0.035*	0.127	*0.026*	0.158	*0.051*	0.176	*0.036*	0.153	*0.065*
ThO_2*	6.75	*1.91*	8.80	*0.49*	7.27	*0.21*	9.56	*0.68*	5.61	*0.46*	9.49	*0.50*	7.83	*1.23*	7.98	*0.99*	7.53	*2.46*
Th/U	8.89	*6.20*	7.96	*1.79*	6.57	*0.40*	41.51	*10.56*	15.09	*1.50*	12.77	*4.47*	13.96	*4.02*	10.08	*4.10*	9.96	*6.77*
Age [Ma]	571	*42*	597	*19*	642	*17*	541	*12*	622	*25*	548	*23*	574	*48*	573	*35*	551	*23*
+/- [Ma]	31	*11*	21	*1*	26	*1*	19	*1*	33	*3*	20	*1*	24	*4*	24	*3*	29	*12*

Table 3 (continued).

Sample	SK1901B		SK1901E		SK1901E		SK1901E		SK1901E		SK1901E		SK1901E		SK1901E		SK1901E	
Grain #	m-106		mnz-#1		mnz-#1		mnz-#1		mnz-#2		mnz-#2		mnz-#2		mnz-#4		mnz-#7	
spot	(with zrn)		core		mantle		rim		core		mantle		rim				core	
	average	*s.d.*	*average*	*s.d.*	*average*	*s.d.*	*average*	*s.d.*	*average*	*s.d.*	*average*	*s.d.*	*average*	*s.d.*	*average*	*s.d.*	*average*	*s.d.*
Wt%	*n=9*		*n=3*		*n=4*		*n=6*		*n=3*		*n=12*		*n=2*		*n=6*		*n=3*	
P_2O_5	27.35	*0.39*	32.79	*0.14*	31.99	*0.49*	31.28	*0.27*	31.55	*0.69*	30.80	*0.57*	31.70	*0.14*	32.33	*0.53*	31.99	*0.15*
SiO_2	0.43	*0.11*	0.76	*0.03*	0.91	*0.21*	1.15	*0.23*	0.93	*0.08*	1.19	*0.32*	0.68	*0.00*	0.33	*0.08*	0.57	*0.05*
CaO	1.40	*0.22*	0.95	*0.05*	0.93	*0.15*	0.83	*0.06*	0.95	*0.02*	0.95	*0.08*	0.68	*0.01*	0.41	*0.08*	0.86	*0.06*
Y_2O_3	0.32	*0.14*	0.05	*0.02*	d.l.		d.l.		0.06	*0.02*	d.l.		d.l.		0.04	*0.02*	0.06	*0.01*
La_2O_3	15.32	*0.46*	16.51	*0.05*	15.90	*0.56*	16.28	*0.21*	15.64	*0.49*	16.36	*0.62*	17.28	*0.02*	16.99	*0.20*	16.27	*0.28*
Ce_2O_3	29.66	*0.72*	30.49	*0.21*	30.81	*0.32*	30.61	*0.21*	30.68	*0.40*	30.54	*0.77*	31.56	*0.08*	32.83	*0.30*	30.70	*0.11*
Pr_2O_3	3.59	*0.18*	3.64	*0.04*	3.59	*0.05*	3.54	*0.08*	3.58	*0.16*	3.48	*0.07*	3.67	*0.03*	3.89	*0.14*	3.65	*0.07*
Nd_2O_3	11.04	*0.33*	11.38	*0.05*	11.38	*0.10*	11.18	*0.36*	11.42	*0.11*	10.68	*0.26*	11.23	*0.04*	12.45	*0.26*	11.41	*0.13*
Sm_2O_3	1.52	*0.29*	1.45	*0.04*	1.26	*0.03*	1.12	*0.19*	1.16	*0.02*	0.89	*0.15*	1.21	*0.13*	1.42	*0.10*	1.49	*0.06*
Gd_2O_3	0.74	*0.17*	0.63	*0.05*	0.42	*0.06*	0.31	*0.14*	0.33	*0.13*	0.21	*0.17*	0.43	*0.06*	0.49	*0.16*	0.60	*0.01*
Dy_2O_3	0.13	*0.05*	d.l.		d.l.		d.l.		d.l.		d.l.		d.l.		d.l.		0.05	*0.05*
Er_2O_3	d.l.		d.l.		d.l.		d.l.		d.l.		d.l.		d.l.		d.l.		0.04	*0.04*
Yb_2O_3	d.l.		d.l.		d.l.		d.l.		d.l.		d.l.		d.l.		d.l.		d.l.	
UO_2	0.542	*0.141*	0.545	*0.030*	0.621	*0.039*	0.608	*0.140*	0.614	*0.012*	0.427	*0.082*	0.484	*0.015*	0.580	*0.022*	0.538	*0.031*
ThO_2	6.473	*1.099*	5.660	*0.261*	6.185	*1.358*	6.633	*0.984*	6.297	*0.369*	7.713	*1.520*	4.640	*0.028*	1.807	*0.684*	4.703	*0.317*
PbO	0.202	*0.031*	0.194	*0.012*	0.208	*0.036*	0.211	*0.022*	0.208	*0.020*	0.212	*0.043*	0.136	*0.001*	0.087	*0.013*	0.167	*0.009*
Total	99.13	*0.76*	105.36	*0.53*	104.60	*0.44*	104.10	*0.40*	103.70	*1.02*	103.77	*0.41*	103.93	*0.12*	104.03	*0.45*	103.36	*0.32*
Cations (O=4)																		
P	0.946	*0.005*	1.008	*0.001*	0.997	*0.011*	0.986	*0.006*	0.994	*0.008*	0.979	*0.012*	0.999	*0.002*	1.012	*0.007*	1.008	*0.003*
Si	0.018	*0.004*	0.028	*0.001*	0.034	*0.008*	0.043	*0.008*	0.035	*0.003*	0.045	*0.012*	0.025	*0.000*	0.012	*0.003*	0.021	*0.002*
Ca	0.061	*0.009*	0.037	*0.002*	0.037	*0.006*	0.033	*0.003*	0.038	*0.002*	0.038	*0.004*	0.027	*0.001*	0.016	*0.003*	0.034	*0.003*
Y	0.007	*0.003*	0.001	*0.000*	0.001	*0.001*	d.l.		0.001	*0.000*	d.l.		d.l.		0.001	*0.000*	0.001	*0.000*
La	0.231	*0.008*	0.221	*0.002*	0.216	*0.007*	0.224	*0.004*	0.215	*0.004*	0.226	*0.008*	0.237	*0.000*	0.232	*0.002*	0.223	*0.003*
Ce	0.444	*0.012*	0.405	*0.003*	0.415	*0.003*	0.417	*0.003*	0.418	*0.004*	0.420	*0.009*	0.430	*0.002*	0.445	*0.005*	0.418	*0.001*
Pr	0.053	*0.003*	0.048	*0.001*	0.048	*0.001*	0.048	*0.001*	0.049	*0.002*	0.048	*0.001*	0.050	*0.001*	0.052	*0.002*	0.050	*0.001*
Nd	0.161	*0.004*	0.148	*0.000*	0.150	*0.001*	0.149	*0.005*	0.152	*0.002*	0.143	*0.003*	0.149	*0.000*	0.164	*0.003*	0.152	*0.001*
Sm	0.021	*0.004*	0.018	*0.001*	0.016	*0.000*	0.014	*0.002*	0.015	*0.000*	0.011	*0.002*	0.015	*0.002*	0.018	*0.001*	0.019	*0.001*
Gd	0.010	*0.002*	0.008	*0.001*	0.005	*0.001*	0.004	*0.002*	0.004	*0.002*	0.003	*0.002*	0.005	*0.001*	0.006	*0.002*	0.007	*0.000*
Dy	0.002	*0.001*	-	-	-	-	-	-	-	-	-	-	-	-	-	-	0.001	*0.001*
Er	-	-	-	-	-	-	-	-	-	-	-	-	-	-	-	-	-	-
Yb	-	-	-	-	-	-	-	-	-	-	-	-	-	-	-	-	-	-
U	0.005	*0.001*	0.004	*0.000*	0.005	*0.000*	0.005	*0.001*	0.005	*0.000*	0.004	*0.001*	0.004	*0.000*	0.005	*0.000*	0.004	*0.000*
Th	0.060	*0.010*	0.047	*0.002*	0.052	*0.012*	0.056	*0.008*	0.053	*0.004*	0.066	*0.013*	0.039	*0.000*	0.015	*0.006*	0.040	*0.003*
Pb	0.002	*0.000*	0.002	*0.000*	0.002	*0.000*	0.002	*0.000*	0.002	*0.000*	0.002	*0.000*	0.001	*0.000*	0.001	*0.000*	0.002	*0.000*
Total	2.028	*0.002*	1.980	*0.001*	1.983	*0.003*	1.985	*0.002*	1.985	*0.004*	1.989	*0.002*	1.987	*0.001*	1.986	*0.004*	1.984	*0.001*
Nd/La	0.376	*0.017*	0.360	*0.002*	0.373	*0.011*	0.358	*0.010*	0.381	*0.008*	0.341	*0.012*	0.339	*0.001*	0.382	*0.009*	0.366	*0.007*
Gd/Nd	0.156	*0.032*	0.130	*0.009*	0.085	*0.012*	0.063	*0.028*	0.068	*0.027*	0.045	*0.035*	0.090	*0.012*	0.093	*0.030*	0.123	*0.003*
ThO_2*	8.28	*1.04*	7.48	*0.36*	8.25	*1.49*	8.65	*0.94*	8.34	*0.41*	9.13	*1.68*	6.24	*0.08*	3.73	*0.66*	6.49	*0.42*
Th/U	13.54	*6.10*	10.63	*0.16*	10.10	*1.59*	12.13	*5.60*	10.49	*0.46*	18.81	*3.99*	9.80	*0.24*	3.20	*1.24*	8.94	*0.12*
Age [Ma]	574	*32*	611	*10*	595	*10*	574	*12*	586	*26*	545	*20*	514	*1*	555	*43*	606	*15*
+/- [Ma]	23	*3*	25	*1*	23	*4*	22	*3*	22	*1*	21	*4*	30	*0*	54	*10*	29	*2*

Table 3 (continued).

Sample	SK1901E		SK1901E		SK1901E		SK1901E		SK1901E		SK1901E		SK1901E		SK1901E		SK1901E	
Grain #	mnz-#7		mnz-#7		mnz-#8		mnz-#10		mnz-#10		mnz-#10		mnz-#10		mnz-#10		mnz-#11	
spot	mantle		rim				core-1		core-2		mantle-1		mantle-2		rim		core	
	average	*s.d.*	*average*	*s.d.*	*average*	*s.d.*	*average*	*s.d.*	*average*	*s.d.*	*average*	*s.d.*	*average*	*s.d.*	*average*	*s.d.*	*average*	*s.d.*
Wt%	*n=3*		*n=3*		*n=6*		*n=5*		*n=4*		*n=11*		*n=6*		*n=7*		*n=13*	
P_2O_5	31.19	*0.36*	31.18	*0.26*	31.11	*0.58*	32.08	*0.23*	31.72	*0.28*	30.90	*0.21*	31.56	*0.38*	31.98	*0.47*	32.07	*0.27*
SiO_2	1.10	*0.03*	0.87	*0.04*	1.03	*0.38*	0.52	*0.01*	0.76	*0.13*	1.29	*0.04*	1.02	*0.13*	0.86	*0.15*	0.74	*0.13*
CaO	1.05	*0.04*	0.93	*0.01*	0.91	*0.06*	0.73	*0.04*	0.93	*0.09*	0.98	*0.04*	0.91	*0.06*	0.84	*0.07*	0.95	*0.05*
Y_2O_3	0.04	*0.04*	0.03	*0.02*	0.04	*0.02*	d.l.		0.04	*0.01*	d.l.		d.l.		d.l.		0.08	*0.03*
La_2O_3	15.47	*0.05*	16.64	*0.08*	16.11	*0.27*	16.51	*0.18*	16.20	*0.19*	16.23	*0.20*	16.76	*0.18*	16.91	*0.20*	15.67	*0.23*
Ce_2O_3	29.87	*0.15*	31.04	*0.09*	30.48	*0.72*	31.52	*0.22*	30.78	*0.13*	30.60	*0.29*	30.98	*0.44*	31.19	*0.66*	30.48	*0.33*
Pr_2O_3	3.61	*0.03*	3.60	*0.11*	3.58	*0.18*	3.74	*0.08*	3.67	*0.07*	3.56	*0.09*	3.59	*0.11*	3.60	*0.07*	3.63	*0.13*
Nd_2O_3	11.16	*0.02*	11.12	*0.07*	11.14	*0.25*	11.78	*0.19*	11.39	*0.13*	10.39	*0.20*	10.68	*0.20*	11.03	*0.17*	11.70	*0.13*
Sm_2O_3	1.21	*0.12*	1.00	*0.12*	1.16	*0.33*	1.33	*0.07*	1.18	*0.11*	0.68	*0.07*	0.86	*0.15*	0.97	*0.10*	1.53	*0.12*
Gd_2O_3	0.40	*0.02*	0.30	*0.16*	0.40	*0.22*	0.42	*0.14*	0.25	*0.10*	0.16	*0.10*	0.11	*0.15*	0.30	*0.09*	0.63	*0.14*
Dy_2O_3	d.l.		d.l.		d.l.		d.l.		d.l.		d.l.		d.l.		d.l.		d.l.	
Er_2O_3	d.l.		d.l.		d.l.		d.l.		d.l.		d.l.		d.l.		d.l.		d.l.	
Yb_2O_3	d.l.		d.l.		d.l.		d.l.		d.l.		d.l.		d.l.		d.l.		d.l.	
UO_2	0.669	*0.014*	0.452	*0.084*	0.508	*0.142*	0.572	*0.016*	0.638	*0.047*	0.225	*0.095*	0.317	*0.056*	0.392	*0.083*	0.621	*0.036*
ThO_2	7.557	*0.085*	6.150	*0.197*	6.903	*1.358*	4.096	*0.162*	5.730	*0.217*	8.452	*0.200*	6.917	*0.377*	5.974	*0.841*	5.864	*0.462*
PbO	0.244	*0.006*	0.171	*0.003*	0.206	*0.038*	0.159	*0.006*	0.193	*0.008*	0.211	*0.013*	0.179	*0.012*	0.166	*0.016*	0.204	*0.012*
Total	103.87	*0.43*	103.78	*0.15*	103.85	*0.47*	103.81	*0.50*	103.76	*0.49*	103.95	*0.36*	104.27	*0.26*	104.49	*0.51*	104.48	*0.40*
Cations (O=4)																		
P	0.986	*0.003*	0.988	*0.005*	0.985	*0.013*	1.008	*0.003*	0.999	*0.005*	0.978	*0.003*	0.991	*0.007*	0.998	*0.008*	1.002	*0.005*
Si	0.041	*0.001*	0.033	*0.001*	0.039	*0.015*	0.019	*0.000*	0.028	*0.005*	0.048	*0.001*	0.038	*0.005*	0.032	*0.006*	0.027	*0.005*
Ca	0.042	*0.001*	0.037	*0.001*	0.037	*0.003*	0.029	*0.002*	0.037	*0.004*	0.039	*0.001*	0.036	*0.002*	0.033	*0.003*	0.038	*0.002*
Y	0.001	*0.001*	0.001	*0.000*	0.001	*0.000*	0.000	*0.001*	0.001	*0.000*	d.l.		d.l.		d.l.		0.001	*0.001*
La	0.213	*0.002*	0.230	*0.002*	0.222	*0.004*	0.226	*0.003*	0.222	*0.003*	0.224	*0.003*	0.229	*0.003*	0.230	*0.002*	0.213	*0.003*
Ce	0.408	*0.005*	0.425	*0.003*	0.417	*0.008*	0.428	*0.002*	0.419	*0.004*	0.419	*0.004*	0.420	*0.007*	0.421	*0.007*	0.412	*0.005*
Pr	0.049	*0.000*	0.049	*0.002*	0.049	*0.002*	0.051	*0.001*	0.050	*0.001*	0.049	*0.001*	0.048	*0.002*	0.048	*0.001*	0.049	*0.002*
Nd	0.149	*0.001*	0.149	*0.001*	0.149	*0.003*	0.156	*0.003*	0.151	*0.002*	0.139	*0.003*	0.141	*0.002*	0.145	*0.002*	0.154	*0.002*
Sm	0.016	*0.002*	0.013	*0.001*	0.015	*0.004*	0.017	*0.001*	0.015	*0.001*	0.009	*0.001*	0.011	*0.002*	0.012	*0.001*	0.019	*0.001*
Gd	0.005	*0.000*	0.004	*0.002*	0.005	*0.003*	0.005	*0.002*	0.003	*0.001*	0.002	*0.001*	0.001	*0.002*	0.004	*0.001*	0.008	*0.002*
Dy	-	-	-	-	-	-	-	-	-	-	-	-	-	-	-	-	-	-
Er	-	-	-	-	-	-	-	-	-	-	-	-	-	-	-	-	-	-
Yb	-	-	-	-	-	-	-	-	-	-	-	-	-	-	-	-	-	-
U	0.006	*0.000*	0.004	*0.001*	0.004	*0.001*	0.005	*0.000*	0.005	*0.000*	0.002	*0.001*	0.003	*0.000*	0.003	*0.001*	0.005	*0.000*
Th	0.064	*0.001*	0.052	*0.002*	0.059	*0.012*	0.035	*0.001*	0.049	*0.002*	0.072	*0.002*	0.058	*0.003*	0.050	*0.007*	0.049	*0.004*
Pb	0.002	*0.000*	0.002	*0.000*	0.002	*0.000*	0.002	*0.000*	0.002	*0.000*	0.002	*0.000*	0.002	*0.000*	0.002	*0.000*	0.002	*0.000*
Total	1.986	*0.002*	1.990	*0.003*	1.988	*0.002*	1.985	*0.002*	1.986	*0.003*	1.987	*0.002*	1.985	*0.002*	1.983	*0.002*	1.984	*0.001*
Nd/La	0.376	*0.002*	0.349	*0.004*	0.361	*0.010*	0.372	*0.006*	0.367	*0.006*	0.334	*0.009*	0.332	*0.008*	0.340	*0.004*	0.390	*0.007*
Gd/Nd	0.083	*0.005*	0.063	*0.034*	0.084	*0.044*	0.082	*0.028*	0.051	*0.020*	0.035	*0.021*	0.023	*0.033*	0.063	*0.019*	0.125	*0.028*
ThO_2*	9.78	*0.13*	7.65	*0.09*	8.59	*1.65*	6.00	*0.21*	7.85	*0.33*	9.20	*0.50*	7.97	*0.47*	7.27	*0.70*	7.93	*0.56*
Th/U	11.55	*0.15*	14.30	*2.99*	14.62	*4.02*	7.32	*0.15*	9.22	*0.56*	41.88	*9.05*	22.77	*3.57*	16.40	*4.72*	9.65	*0.46*
Age [Ma]	587	*8*	529	*2*	567	*33*	625	*13*	579	*4*	542	*17*	531	*20*	538	*15*	606	*11*
+/- [Ma]	19	*0*	24	*0*	22	*3*	31	*1*	24	*1*	20	*1*	23	*1*	26	*2*	24	*2*

Table 3 (continued).

Sample	SK1901E		SK1901E		SK1901E		SK1901E		SK1901E		SK1901E		SK1901E		SK1901E	
Grain #	mnz-#11		mnz-#11		mnz-#11		mnz-#19		mnz-#19		mnz-#24		mnz-#24		mnz-#24	
spot	mantle-1		mantle-2		rim		core		rim		core		mantle-1		rim	
	average	*s.d.*	*average*	*s.d.*	*average*	*s.d.*	*average*	*s.d.*	*average*	*s.d.*	*average*	*s.d.*	*average*	*s.d.*	*average*	*s.d.*
Wt%	*n=11*		*n=9*		*n=12*		*n=13*		*n=5*		*n=10*		*n=9*		*n=7*	
P_2O_5	31.08	*0.23*	31.27	*0.17*	31.93	*0.24*	31.79	*0.24*	30.03	*0.37*	31.48	*0.66*	30.70	*0.48*	31.81	*0.31*
SiO_2	1.34	*0.05*	1.17	*0.05*	0.79	*0.03*	0.76	*0.09*	1.66	*0.18*	0.82	*0.20*	1.31	*0.26*	0.51	*0.05*
CaO	1.00	*0.03*	0.89	*0.02*	0.92	*0.04*	0.94	*0.11*	1.00	*0.05*	0.96	*0.18*	0.98	*0.04*	0.51	*0.05*
Y_2O_3	d.l.		d.l.		d.l.		d.l.		d.l.		d.l.		d.l.		d.l.	
La_2O_3	15.80	*0.27*	16.52	*0.10*	16.65	*0.15*	16.20	*0.26*	15.61	*0.26*	16.39	*0.47*	16.22	*0.55*	17.24	*0.24*
Ce_2O_3	30.55	*0.31*	31.36	*0.24*	31.22	*0.30*	30.93	*0.44*	29.58	*0.24*	30.79	*0.54*	30.21	*0.67*	32.01	*0.30*
Pr_2O_3	3.52	*0.10*	3.49	*0.14*	3.62	*0.07*	3.64	*0.14*	3.44	*0.11*	3.61	*0.11*	3.51	*0.11*	3.68	*0.09*
Nd_2O_3	10.61	*0.13*	10.56	*0.16*	11.05	*0.17*	11.34	*0.22*	10.39	*0.15*	11.12	*0.43*	10.47	*0.27*	11.89	*0.25*
Sm_2O_3	0.81	*0.07*	0.76	*0.06*	1.01	*0.07*	1.11	*0.10*	0.78	*0.10*	1.09	*0.24*	0.81	*0.15*	1.30	*0.12*
Gd_2O_3	0.21	*0.12*	0.15	*0.10*	0.29	*0.10*	0.28	*0.13*	0.16	*0.09*	0.29	*0.17*	0.22	*0.09*	0.44	*0.13*
Dy_2O_3	d.l.		d.l.		d.l.		d.l.		d.l.		0.01	*0.01*	0.01	*0.02*	0.02	*0.02*
Er_2O_3	d.l.		d.l.		d.l.		d.l.		d.l.		0.02	*0.03*	0.01	*0.02*	0.01	*0.01*
Yb_2O_3	d.l.		d.l.		d.l.		d.l.		d.l.		d.l.		d.l.		d.l.	
UO_2	0.417	*0.121*	0.361	*0.014*	0.424	*0.053*	0.596	*0.056*	0.735	*0.087*	0.559	*0.145*	0.470	*0.257*	0.478	*0.052*
ThO_2	8.594	*0.225*	7.550	*0.111*	6.133	*0.126*	5.751	*0.688*	9.452	*0.694*	6.066	*1.189*	8.261	*1.015*	3.300	*0.344*
PbO	0.232	*0.009*	0.201	*0.006*	0.172	*0.006*	0.192	*0.020*	0.289	*0.024*	0.194	*0.029*	0.229	*0.049*	0.111	*0.006*
Total	104.47	*0.43*	104.57	*0.50*	104.50	*0.64*	103.84	*0.42*	103.36	*0.55*	103.69	*0.72*	103.72	*0.58*	103.55	*0.43*
Cations (O=4)																
P	0.978	*0.004*	0.983	*0.003*	0.998	*0.003*	0.999	*0.003*	0.963	*0.007*	0.994	*0.011*	0.976	*0.010*	1.004	*0.005*
Si	0.050	*0.002*	0.044	*0.002*	0.029	*0.001*	0.028	*0.003*	0.063	*0.007*	0.031	*0.008*	0.049	*0.010*	0.019	*0.002*
Ca	0.040	*0.001*	0.036	*0.001*	0.036	*0.002*	0.037	*0.005*	0.041	*0.002*	0.038	*0.007*	0.039	*0.002*	0.020	*0.002*
Y	d.l.		d.l.		-	-	-	-	-	-	-	-	-	-	-	
La	0.217	*0.003*	0.226	*0.002*	0.227	*0.002*	0.222	*0.004*	0.218	*0.003*	0.226	*0.006*	0.225	*0.007*	0.237	*0.003*
Ce	0.416	*0.004*	0.426	*0.003*	0.422	*0.004*	0.421	*0.006*	0.410	*0.002*	0.421	*0.007*	0.415	*0.008*	0.437	*0.005*
Pr	0.048	*0.001*	0.047	*0.002*	0.049	*0.001*	0.049	*0.002*	0.047	*0.001*	0.049	*0.001*	0.048	*0.001*	0.050	*0.001*
Nd	0.141	*0.002*	0.140	*0.002*	0.146	*0.002*	0.150	*0.003*	0.141	*0.001*	0.148	*0.005*	0.140	*0.004*	0.158	*0.003*
Sm	0.010	*0.001*	0.010	*0.001*	0.013	*0.001*	0.014	*0.001*	0.010	*0.001*	0.014	*0.003*	0.010	*0.002*	0.017	*0.002*
Gd	0.003	*0.001*	0.002	*0.001*	0.004	*0.001*	0.003	*0.002*	0.002	*0.001*	0.004	*0.002*	0.003	*0.001*	0.005	*0.002*
Dy	-	-	-	-	-	-	-	-	-	-	0.000	*0.000*	0.000	*0.000*	0.000	*0.000*
Er	-	-	-	-	-	-	-	-	-	-	0.000	*0.000*	0.000	*0.000*	0.000	*0.000*
Yb	-	-	-	-	-	-	-	-	-	-	-		-		-	
U	0.003	*0.001*	0.003	*0.000*	0.003	*0.000*	0.005	*0.000*	0.006	*0.001*	0.005	*0.001*	0.004	*0.002*	0.004	*0.000*
Th	0.073	*0.002*	0.064	*0.001*	0.052	*0.001*	0.049	*0.006*	0.081	*0.006*	0.052	*0.010*	0.071	*0.009*	0.028	*0.003*
Pb	0.002	*0.000*	0.002	*0.000*	0.002	*0.000*	0.002	*0.000*	0.003	*0.000*	0.002	*0.000*	0.002	*0.001*	0.001	*0.000*
Total	1.985	*0.002*	1.986	*0.002*	1.985	*0.002*	1.985	*0.002*	1.988	*0.001*	1.987	*0.003*	1.988	*0.002*	1.986	*0.002*
Nd/La	0.350	*0.008*	0.334	*0.004*	0.346	*0.007*	0.365	*0.005*	0.347	*0.001*	0.354	*0.015*	0.337	*0.014*	0.360	*0.009*
Gd/Nd	0.047	*0.026*	0.034	*0.022*	0.060	*0.021*	0.057	*0.026*	0.036	*0.020*	0.061	*0.035*	0.049	*0.020*	0.086	*0.024*
ThO_2*	9.98	*0.36*	8.75	*0.13*	7.54	*0.13*	7.73	*0.85*	11.89	*0.88*	7.93	*1.25*	9.82	*1.72*	4.88	*0.22*
Th/U	22.91	*7.10*	21.39	*0.81*	15.03	*2.05*	9.86	*0.55*	13.27	*1.52*	12.02	*4.86*	22.37	*10.00*	7.23	*1.79*
Age [Ma]	549	*10*	543	*12*	537	*13*	587	*19*	572	*7*	580	*34*	546	*25*	537	*21*
+/- [Ma]	18	*1*	21	*0*	24	*0*	24	*3*	16	*1*	24	*4*	19	*3*	39	*2*

Table 4. Chemical compositions of monazites in pelitic gneiss (21409) from Mt. Riiser-Larsen, Napier Complex, East Antarctica.

Sample	21409	21409	21409	21409	21409	21409	21409	21409	21409	21409	21409	21409	21409	21409	21409	21409	21409	21409	21409
Grain #	m1	m1	m1	m1	m1	m2	m2	m2	m2	m2	m3	m4	m4	m4	m4	m5	m5	m6	m7
spot	17	18	19	20	21	22	23	24	25	26	27	28	29	30	31	32	33	34	35
	EA	*EA*	*EA*	*EA*	*EA*	*EA*	*EA*	*EA*	*EA*	*EA*	*	*EA*	*EA*	*EA*	*EA*	*EA*	*EA*	*I*	*IA*
Wt%																			
P_2O_5	30.07	29.82	29.80	29.31	29.80	29.85	29.76	30.65	29.31	30.19	29.25	30.10	30.58	29.94	30.64	30.48	30.23	30.00	30.26
SiO_2	1.19	0.97	1.13	1.19	1.56	0.78	1.02	0.57	1.54	0.62	1.19	0.92	0.53	1.30	0.59	0.62	0.85	0.96	0.86
CaO	1.30	1.20	1.30	1.22	1.31	1.07	1.09	1.07	1.26	1.09	1.30	1.32	1.17	1.19	1.13	1.16	1.08	1.68	1.31
Y_2O_3	d.l.	0.04	0.04	d.l.	0.04	d.l.	d.l.	0.06	d.l.	0.03	0.05	0.06	0.08	d.l.	0.04	0.05	0.04	0.08	0.04
La_2O_3	14.63	13.79	13.71	13.99	13.95	14.93	14.61	14.80	13.61	14.90	13.59	14.23	14.79	14.23	14.69	15.17	14.36	13.18	14.03
Ce_2O_3	32.37	32.66	32.31	32.37	32.55	31.96	31.69	32.59	31.92	32.19	32.33	32.37	32.21	32.23	31.81	32.20	32.44	30.57	32.10
Pr_2O_3	2.98	3.07	3.06	3.13	3.12	2.97	2.94	3.09	3.04	2.94	3.17	3.14	2.97	3.08	2.96	2.99	3.06	3.05	2.98
Nd_2O_3	10.78	11.61	11.37	11.23	11.21	11.52	11.65	11.81	11.06	11.57	11.30	11.23	11.58	11.32	11.69	11.64	11.99	11.43	11.60
Sm_2O_3	0.97	0.94	0.85	0.84	0.87	1.69	1.84	1.68	0.81	1.74	0.85	1.09	1.76	1.05	1.85	1.71	1.31	1.36	1.20
Gd_2O_3	0.25	0.25	0.24	0.20	0.19	0.65	0.72	0.66	0.19	0.67	0.20	0.31	0.68	0.31	0.80	0.69	0.43	0.43	0.44
Dy_2O_3	0.14	0.17	0.18	0.16	0.20	0.13	0.14	0.13	0.19	0.14	0.13	0.15	0.13	0.18	0.12	0.13	0.10	0.19	0.15
Er_2O_3	d.l.	d.l.	d.l.	d.l.	d.l.	d.l.	d.l.	d.l.	d.l.	d.l.	d.l.	d.l.	d.l.	d.l.	d.l.	d.l.	d.l.	d.l.	d.l.
Yb_2O_3	d.l.	d.l.	d.l.	d.l.	d.l.	d.l.	d.l.	d.l.	d.l.	d.l.	d.l.	d.l.	d.l.	d.l.	d.l.	d.l.	d.l.	d.l.	d.l.
UO_2	0.610	0.300	0.312	0.334	0.325	0.385	0.385	0.225	0.293	0.370	0.337	0.680	0.310	0.505	0.391	0.353	0.308	0.812	0.797
ThO_2	7.310	7.360	7.750	8.000	8.020	5.850	5.780	5.550	9.330	5.660	7.920	7.060	6.000	7.420	5.790	5.960	6.200	7.770	6.320
PbO	0.411	0.502	0.572	0.791	0.627	0.541	0.589	0.205	0.906	0.403	0.903	0.585	0.285	0.751	0.479	0.242	0.213	1.231	0.878
Total	103.05	102.68	102.63	102.77	103.78	102.35	102.22	103.08	103.51	102.51	102.53	103.23	103.09	103.54	102.97	103.40	102.61	102.77	102.97
Cations (O=4)																			
P	0.967	0.969	0.966	0.957	0.955	0.973	0.969	0.985	0.950	0.980	0.957	0.971	0.984	0.963	0.986	0.980	0.977	0.972	0.976
Si	0.045	0.037	0.043	0.046	0.059	0.030	0.039	0.021	0.059	0.024	0.046	0.035	0.020	0.050	0.022	0.024	0.032	0.037	0.033
Ca	0.053	0.049	0.053	0.050	0.053	0.044	0.045	0.044	0.052	0.045	0.054	0.054	0.047	0.048	0.046	0.047	0.044	0.069	0.054
Y	-	0.001	0.001	-	0.001	-	-	0.001	-	0.001	0.001	0.001	0.002	-	0.001	0.001	0.001	0.002	0.001
La	0.205	0.195	0.194	0.199	0.195	0.212	0.207	0.207	0.192	0.211	0.194	0.200	0.207	0.199	0.206	0.212	0.202	0.186	0.197
Ce	0.450	0.459	0.453	0.457	0.451	0.451	0.446	0.453	0.447	0.452	0.458	0.451	0.448	0.448	0.443	0.448	0.453	0.428	0.448
Pr	0.041	0.043	0.043	0.044	0.043	0.042	0.041	0.043	0.042	0.041	0.045	0.044	0.041	0.043	0.041	0.041	0.043	0.043	0.041
Nd	0.146	0.159	0.155	0.155	0.151	0.158	0.160	0.160	0.151	0.158	0.156	0.153	0.157	0.154	0.159	0.158	0.163	0.156	0.158
Sm	0.013	0.012	0.011	0.011	0.011	0.022	0.024	0.022	0.011	0.023	0.011	0.014	0.023	0.014	0.024	0.022	0.017	0.018	0.016
Gd	0.003	0.003	0.003	0.003	0.002	0.008	0.009	0.008	0.002	0.009	0.003	0.004	0.009	0.004	0.010	0.009	0.005	0.005	0.006
Dy	0.002	0.002	0.002	0.002	0.002	0.002	0.002	0.002	0.002	0.002	0.002	0.002	0.002	0.002	0.001	0.002	0.001	0.002	0.002
Er	0.000	0.000	0.000	0.000	0.000	0.000	0.000	0.000	0.000	0.000	0.000	0.000	0.000	0.000	0.000	0.000	0.000	0.000	0.000
Yb	-	-	-	-	-	-	-	-	-	-	-	-	-	-	-	-	-	-	-
U	-	-	-	-	-	-	-	-	-	-	-	-	-	-	-	-	-	-	-
Th	0.063	0.064	0.068	0.070	0.069	0.051	0.051	0.048	0.081	0.049	0.070	0.061	0.052	0.064	0.050	0.051	0.054	0.068	0.055
Pb	0.004	0.005	0.006	0.008	0.006	0.006	0.006	0.002	0.009	0.004	0.009	0.006	0.003	0.008	0.005	0.002	0.002	0.013	0.009
Total	1.998	2.001	2.001	2.004	2.002	2.003	2.004	1.997	2.002	2.000	2.008	2.002	1.998	2.001	1.998	2.000	1.998	2.006	2.001
Nd/La	0.384	0.439	0.433	0.419	0.419	0.402	0.416	0.416	0.424	0.405	0.434	0.412	0.408	0.415	0.415	0.400	0.436	0.452	0.431
Gd/Nd	0.055	0.051	0.049	0.042	0.039	0.131	0.144	0.130	0.041	0.135	0.042	0.063	0.136	0.064	0.159	0.139	0.083	0.087	0.088
ThO_2*	9.42	8.43	8.87	9.26	9.20	7.27	7.22	6.31	10.44	6.97	9.24	9.50	7.06	9.31	7.21	7.16	7.24	11.07	9.40
Th/U	12.25	25.10	25.44	24.53	25.21	15.52	15.35	25.24	32.62	15.65	24.02	10.61	19.79	15.02	15.15	17.25	20.55	9.78	8.10
Age [Ma]	1018	1377	1485	1944	1566	1704	1860	761	1975	1338	2212	1423	942	1842	1530	792	693	2498	2118
+/- [Ma]	14	15	15	14	14	18	18	21	13	19	14	14	18	14	18	18	18	12	14

d.l.: below detection limit

*I: inclusion in garnet or sillimanite, IA: inclusion in altered garnet, EA: edge of altered garnet, BS: with biotite-sillimanite aggregate, *: other*

Table 4 (continued).

Sample	21409	21409	21409	21409	21409	21409	21409	21409	21409	21409	21409	21409	21409	21409	21409	21409	21409	21409	21409
Grain #	m7	m7	m7	m7	m8	m8	m8	m9	m10	m10	m10	m11	m11	m11	m11	m12	m12	m12	m13
spot	36	37	38	39	40	41	42	43	44	45	46	47	48	49	50	51	52	53	54
	IA	*IA*	*IA*	*IA*	*	*	*	*	*BS*	*BS*	*BS*	*I*	*I*	*I*	*I*	*	*	*	*
Wt%																			
P_2O_5	30.17	29.87	29.07	29.24	29.37	29.90	28.68	31.15	30.48	30.36	30.34	29.53	29.53	28.56	30.19	29.19	29.00	30.06	28.16
SiO_2	0.82	1.01	1.40	1.03	1.47	1.31	1.62	0.35	0.29	0.22	0.25	1.14	1.23	1.31	1.20	1.65	1.73	0.94	2.24
CaO	1.30	1.32	1.30	1.32	1.10	0.91	1.12	0.07	0.25	0.24	0.23	1.61	1.43	1.36	1.56	1.21	1.11	0.94	1.30
Y_2O_3	d.l.	0.06	0.09	0.05	d.l.	d.l.	0.05	d.l.	d.l.	d.l.	0.04	0.03	d.l.	0.07	d.l.	d.l.	d.l.	0.08	d.l.
La_2O_3	13.91	13.57	13.52	13.57	13.32	13.83	13.22	16.62	15.18	15.62	15.76	12.31	12.78	12.82	12.60	13.10	13.44	14.46	12.51
Ce_2O_3	32.05	32.05	31.62	32.27	32.48	33.18	32.27	32.89	34.10	34.22	34.35	31.12	31.48	31.73	31.53	31.73	32.36	32.18	31.37
Pr_2O_3	3.05	3.08	3.01	3.07	3.20	3.28	3.10	3.20	3.43	3.38	3.43	3.14	3.19	3.15	3.16	3.19	3.22	3.03	3.12
Nd_2O_3	11.75	11.71	11.30	11.67	11.34	12.10	11.24	16.49	15.61	15.21	15.30	12.20	12.08	11.96	12.18	11.84	11.39	11.96	11.31
Sm_2O_3	1.32	1.16	0.90	0.95	0.79	0.79	0.77	1.59	1.25	1.23	1.26	1.07	1.01	0.98	1.11	1.04	0.79	1.69	0.80
Gd_2O_3	0.38	0.30	0.26	0.24	0.11	0.16	0.15	0.25	0.21	0.24	0.17	0.29	0.28	0.26	0.28	0.18	0.21	0.70	0.23
Dy_2O_3	0.14	0.16	0.16	0.18	0.21	0.16	0.19	d.l.	d.l.	d.l.	d.l.	0.18	0.16	0.18	0.17	0.16	0.18	0.16	0.25
Er_2O_3	d.l.	d.l.	d.l.	d.l.	d.l.	d.l.	d.l.	d.l.	d.l.	d.l.	d.l.	d.l.	d.l.	d.l.	d.l.	d.l.	d.l.	d.l.	d.l.
Yb_2O_3	d.l.	d.l.	d.l.	d.l.	d.l.	d.l.	d.l.	d.l.	d.l.	d.l.	d.l.	d.l.	d.l.	d.l.	d.l.	d.l.	d.l.	d.l.	d.l.
UO_2	0.879	0.728	0.341	0.355	0.186	0.207	0.184	0.138	0.228	0.190	0.199	0.265	0.266	0.246	0.265	0.256	0.194	0.298	0.182
ThO_2	6.360	7.230	8.840	7.550	8.890	7.080	9.050	0.114	1.121	0.994	0.957	8.630	8.470	8.640	8.560	8.820	8.840	5.710	11.500
PbO	0.938	0.740	0.811	0.949	0.524	0.478	0.523	0.045	0.165	0.143	0.127	1.065	1.040	1.044	1.065	0.706	0.819	0.603	0.912
Total	103.09	103.00	102.65	102.46	102.99	103.43	102.16	102.92	102.36	102.06	102.44	102.59	102.96	102.32	103.88	103.10	103.32	102.81	103.89
Cations (O=4)																			
P	0.975	0.968	0.951	0.959	0.954	0.962	0.943	0.997	0.989	0.990	0.987	0.962	0.960	0.944	0.966	0.948	0.942	0.972	0.919
Si	0.031	0.038	0.054	0.040	0.056	0.050	0.063	0.013	0.011	0.008	0.010	0.044	0.047	0.051	0.045	0.063	0.066	0.036	0.086
Ca	0.053	0.054	0.054	0.055	0.045	0.037	0.047	0.003	0.010	0.010	0.010	0.066	0.059	0.057	0.063	0.050	0.045	0.039	0.054
Y	-	0.001	0.002	0.001	-	-	0.001	-	-	-	0.001	0.001	-	0.001	-	-	-	0.002	-
La	0.196	0.192	0.193	0.194	0.188	0.194	0.189	0.232	0.215	0.222	0.223	0.175	0.181	0.185	0.176	0.185	0.190	0.204	0.178
Ce	0.448	0.449	0.447	0.458	0.456	0.462	0.459	0.455	0.479	0.482	0.483	0.438	0.442	0.454	0.436	0.445	0.455	0.450	0.443
Pr	0.042	0.043	0.042	0.043	0.045	0.045	0.044	0.044	0.048	0.047	0.048	0.044	0.045	0.045	0.044	0.045	0.045	0.042	0.044
Nd	0.160	0.160	0.156	0.161	0.155	0.164	0.156	0.223	0.214	0.209	0.210	0.168	0.166	0.167	0.164	0.162	0.156	0.163	0.156
Sm	0.017	0.015	0.012	0.013	0.010	0.010	0.010	0.021	0.017	0.016	0.017	0.014	0.013	0.013	0.014	0.014	0.010	0.022	0.011
Gd	0.005	0.004	0.003	0.003	0.001	0.002	0.002	0.003	0.003	0.003	0.002	0.004	0.003	0.003	0.004	0.002	0.003	0.009	0.003
Dy	0.002	0.002	0.002	0.002	0.003	0.002	0.002	0.000	0.000	0.000	0.000	0.002	0.002	0.002	0.002	0.002	0.002	0.002	0.003
Er	0.000	0.000	0.000	0.000	0.000	0.000	0.000	-	-	-	-	0.000	0.000	0.000	0.000	0.000	0.000	0.000	0.000
Yb	-	-	-	-	-	-	-	-	-	-	-	-	-	-	-	-	-	-	-
U	-	-	-	-	-	-	-	-	-	-	-	-	-	-	-	-	-	-	-
Th	0.055	0.063	0.078	0.067	0.078	0.061	0.080	0.001	0.010	0.009	0.008	0.076	0.074	0.077	0.074	0.077	0.077	0.050	0.101
Pb	0.010	0.008	0.008	0.010	0.005	0.005	0.005	0.000	0.002	0.001	0.001	0.011	0.011	0.011	0.011	0.007	0.008	0.006	0.009
Total	2.002	2.003	2.005	2.009	1.999	1.998	2.003	1.994	1.999	2.000	2.001	2.007	2.006	2.012	2.002	2.003	2.003	1.998	2.008
Nd/La	0.441	0.450	0.436	0.449	0.444	0.456	0.443	0.518	0.536	0.508	0.506	0.517	0.493	0.487	0.504	0.471	0.442	0.431	0.472
Gd/Nd	0.075	0.060	0.054	0.048	0.023	0.031	0.032	0.036	0.032	0.036	0.027	0.056	0.053	0.050	0.053	0.035	0.043	0.136	0.048
ThO_2*	9.78	9.92	10.12	8.97	9.55	7.82	9.70	0.62	1.98	1.71	1.69	9.70	9.54	9.63	9.63	9.76	9.57	6.85	12.17
Th/U	7.40	10.16	26.48	21.73	48.83	34.94	50.35	0.84	5.04	5.36	4.92	33.27	32.61	35.89	33.04	35.27	46.70	19.56	64.79
Age [Ma]	2172	1710	1831	2384	1272	1411	1250	1659	1905	1905	1721	2467	2452	2439	2484	1660	1949	2004	1717
+/- [Ma]	13	13	13	15	14	17	13	211	66	77	77	14	14	14	14	13	14	19	11

*I: inclusion in garnet or sillimanite, IA: inclusion in altered garnet, EA: edge of altered garnet, BS: with biotite-sillimanite aggregate, *: other*

Table 5. Summary of EMP monazite ages of garnet-bearing pelitic gneisses from the Lützow-Holm Complex and the Napier Complex, East Antarctica.

Sample	Age populations	Total # of analytical spots and monazite grains in a thin section	Calculated age*	Type**
Skallen, Lützow-Holm Complex				
2303A	550-520 Ma	27 spots on 2 monazite grains	547+/-6 Ma	A
1901A	560-530 Ma	74 spots on 9 monazite grains	540+/-5 Ma	A
1901B	640-530 Ma	149 spots on 23 monazite grains	553+/-6 Ma	B
1901E	630-510 Ma	172 spots on 29 monazite grains	543+/-4 Ma	B
Mt. Riiser-Larsen, Napier Complex				
21409	2500-700 Ma	38 spots on 13 monazite grains	2470+/-30 Ma	

* Weighted average age (2-sigma error) calculated for major age group.
** See text for detail of type A and B classification.

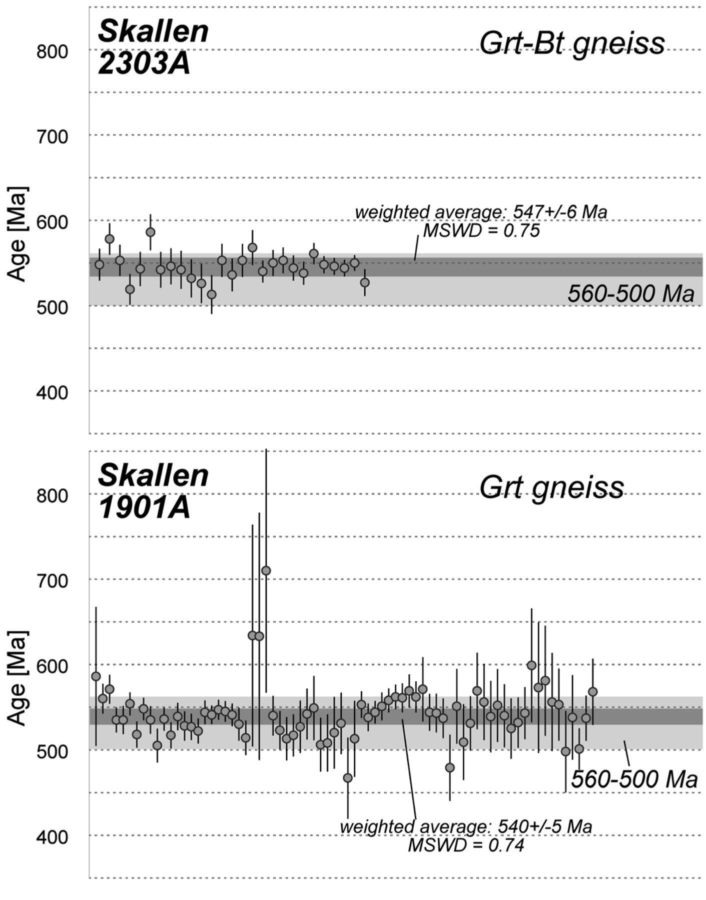

Fig. 6. EMP monazite U-Th-Pb apparent ages of garnet-biotite-bearing metapelites from Skallen, Lützow-Holm Complex and garnet-sillimanite gneiss from Mt. Riiser-Larsen, Napier Complex. Errors are at 1-sigma (67% confidence) uncertainty.

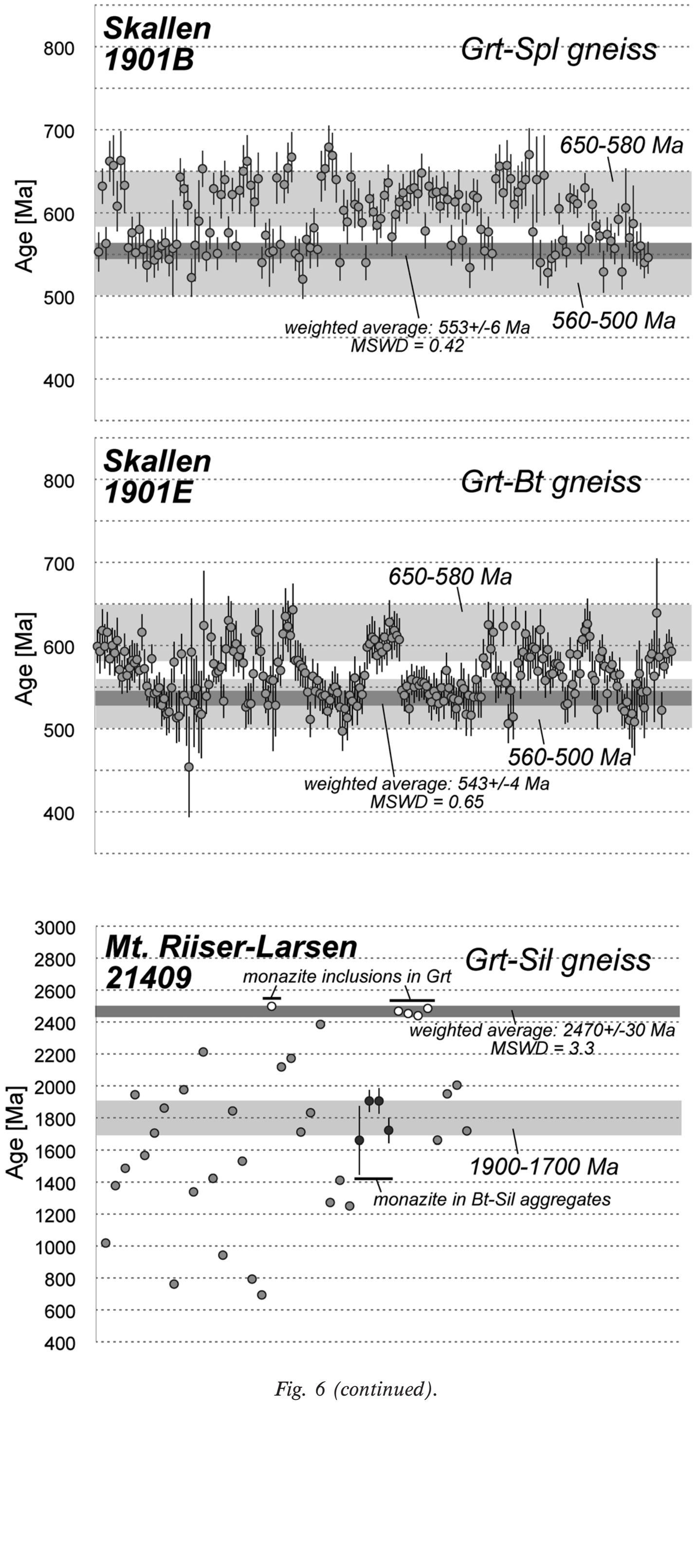

Fig. 6 (continued).

and 1901A: hereafter named as *group-A*) yield a single 560–500 Ma age population, whereas the other two samples (1901B and 1901E: named as *group-B*) suggest the presence of at least two (560–500 Ma and 650–580 Ma) age populations (Fig. 6). The weighted averages of the younger age populations (540±5 Ma~553±6 Ma; mainly from higher-BEI luminescence rim or structureless or homogeneous grain) are consistent in all four samples (Table 5 and Fig. 6). Weighted averages of older ages in group-B samples could not be statistically defined, although age data lie within a range of 650–

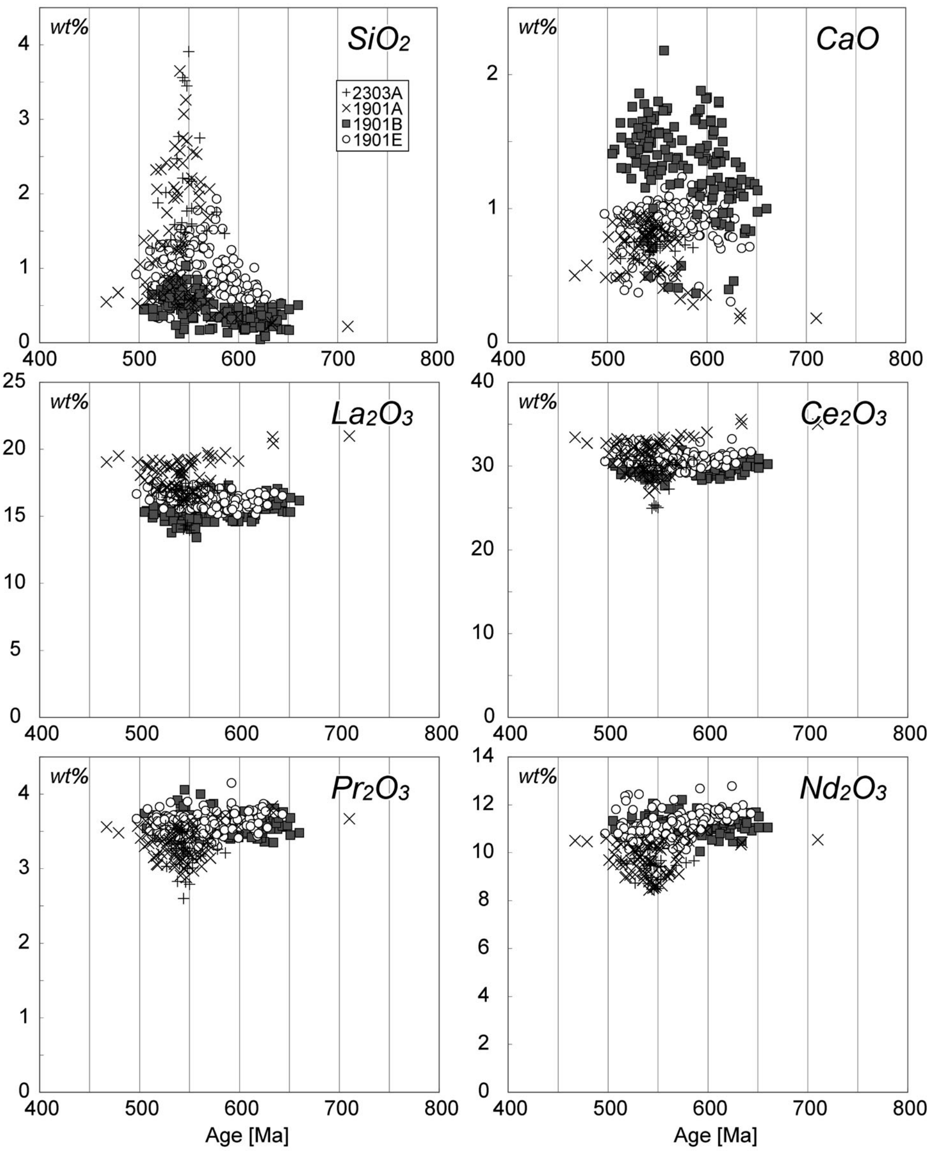

Fig. 7. EMP U-Th-Pb ages versus chemical composition of monazite in metapelite from Skallen.

580 Ma, in many cases, from a lower-BEI luminescence core or structureless or homogeneous grain. The numbers of monazite grains found in one thin section are different between group-A (2 and 9 grains in each sample; Table 5) and group-B samples (23 and 29 grains in each); hence, the *group-A* samples have numbers of monazite grains less than 1/10~1/3 of *group-B* samples.

Age-chemistry relations of analyzed monazite are shown in Fig. 7. Monazite has a relatively large compositional variation within each sample. For *group-A* samples

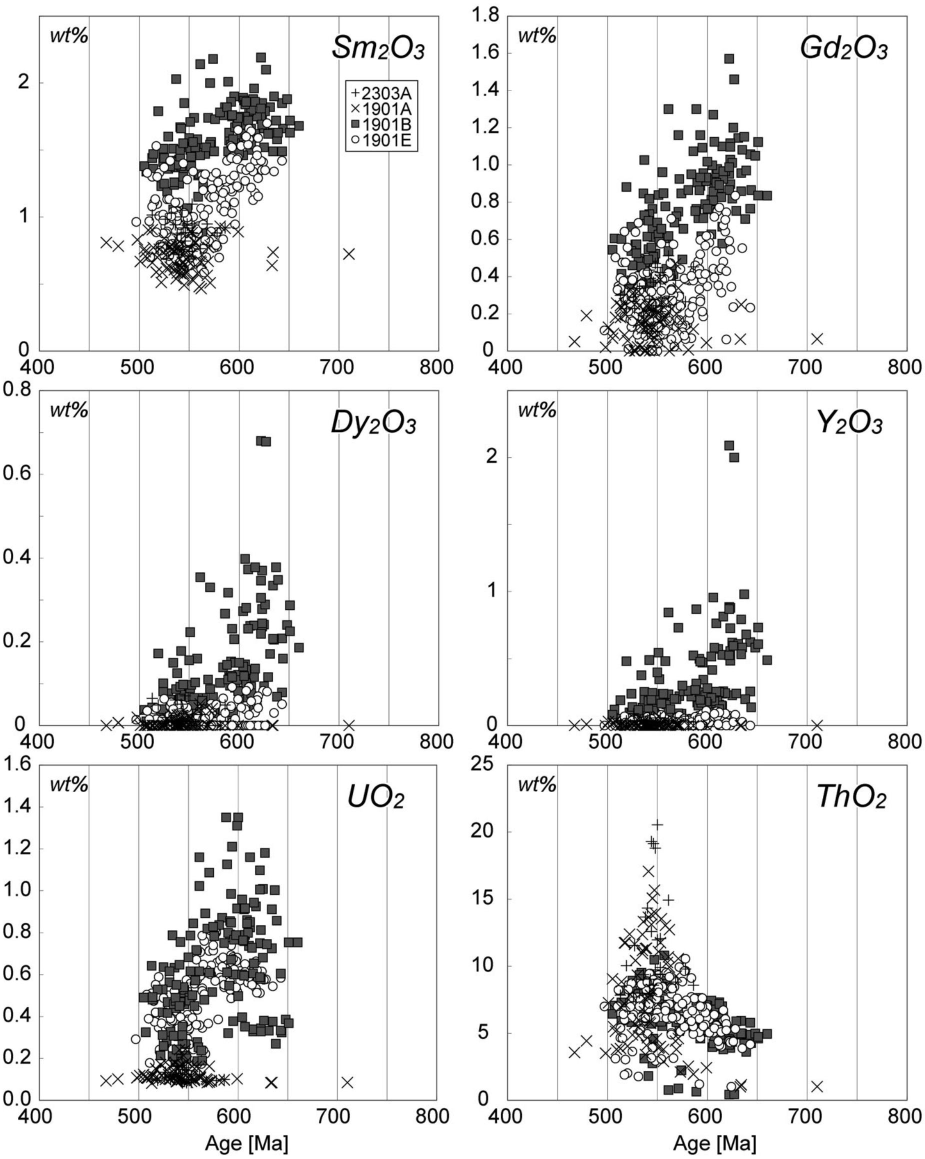

Fig. 7 (continued).

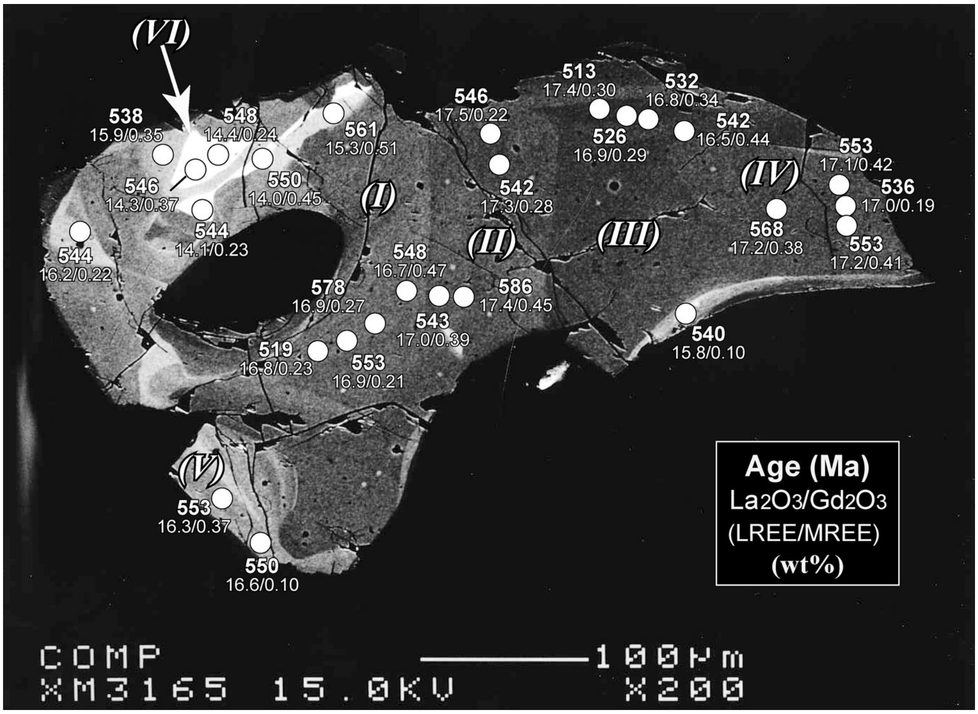

Fig. 8. Backscattered-electron image (BEI) of monazite grain-#1, sample 2303A (group-A), from Skallen. Six distinct zones give consistent c. 550 Ma ages.

(2303A and 1901A), backscattered electron images of relatively coarse monazite grains (*e.g.,* grain #1 of 2303A; Fig. 8) show five distinct zones (from inner zone (I) to outer zone (V)), along with a bright-BEI patchy zone (VI). Compositional changes from zone-(I) to zone-(VI) are mainly controlled by substitution between $ThSiO_4$ (huttonite) and (La, Ce, Pr, Nd)PO_4 (REE monazite), with brighter BEI zones corresponding to higher huttonite contents. No association, however, is observed between age and monazite composition.

For *group-B* samples (1901B and 1901E), slight compositional differences between 650–580 Ma and 560–500 Ma monazites can be seen: older (650–580 Ma) monazite has higher Nd, Sm, Gd, Dy and lower Si (and possibly Ca and Th) contents than younger (560–500 Ma) domains and/or grains (Fig. 7). Compositional change of monazite from 650–580 Ma to 560–500 Ma corresponds to the following substitutions among the end member components (monazite: (La, Ce)PO_4, huttonite: $ThSiO_4$, brabantite: ThCa $(PO_4)_2$) from left to right:

Fig. 9 (opposite). Modes of occurrence of monazite grains (A, C) and BEI of monazites (B, D–H) in garnet-biotite-bearing metapelitic (group-B) samples from Skallen. Bright symbol indicates 560–500 Ma domains/grains and dark symbol is older 650–580 Ma domains/grains. A. Monazite (grain-#4) on garnet edge. Plane-polarized light. B. BEI of monazite grain-#4. C. Fine-grained monazite (grain-#102) enclosed within spinel. Plane-polarized light. D. BEI of monazite grain-#102. E-F-G-H. BEI of monazite grains.

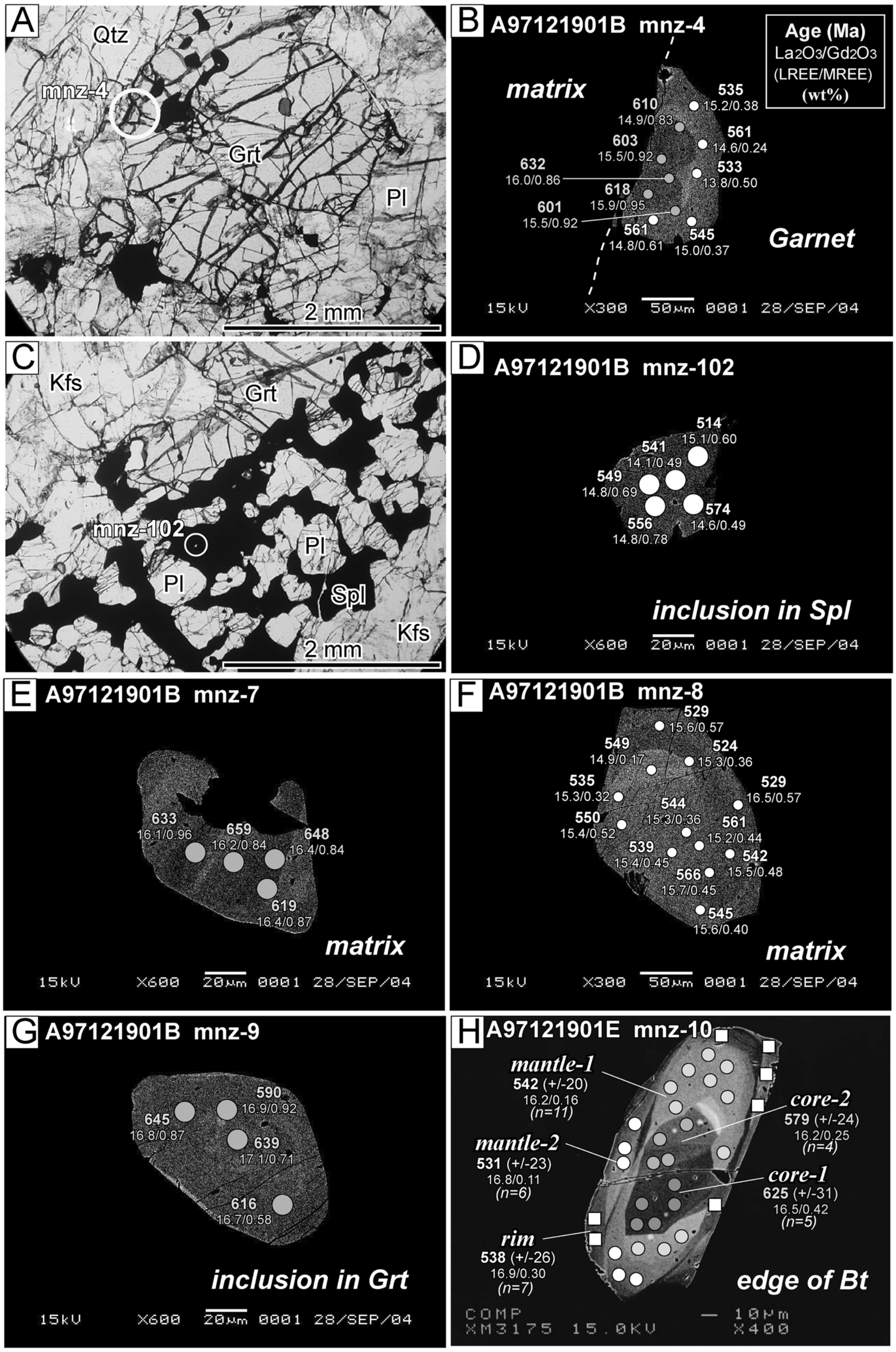
A
Qtz
mnz-4
Grt
Pl
2 mm
B
A97121901B mnz-4
Age (Ma)
La2O3/Gd2O3
(LREE/MREE)
(wt%)
matrix
535
15.2/0.38
610
14.9/0.83
561
14.6/0.24
603
15.5/0.92
632
16.0/0.86
533
13.8/0.50
618
15.9/0.95
601
15.5/0.92
561
14.8/0.61
545
15.0/0.37
Garnet
15kV X300 50μm 0001 28/SEP/04
C
Kfs
Grt
mnz-102
Pl
Pl
Spl
Kfs
2 mm
D
A97121901B mnz-102
514
15.1/0.60
541
14.1/0.49
549
14.8/0.69
574
14.6/0.49
556
14.8/0.78
inclusion in Spl
15kV X600 20μm 0001 28/SEP/04
E
A97121901B mnz-7
633
16.1/0.96
659
16.2/0.84
648
16.4/0.84
619
16.4/0.87
matrix
15kV X600 20μm 0001 28/SEP/04
F
A97121901B mnz-8
529
15.6/0.57
549
14.9/0.17
524
15.3/0.36
535
15.3/0.32
529
16.5/0.57
544
15.3/0.36
550
15.4/0.52
561
15.2/0.44
539
15.4/0.45
542
15.5/0.48
566
15.7/0.45
545
15.6/0.40
matrix
15kV X300 50μm 0001 28/SEP/04
G
A97121901B mnz-9
590
16.9/0.92
645
16.8/0.87
639
17.1/0.71
616
16.7/0.58
inclusion in Grt
15kV X600 20μm 0001 28/SEP/04
H
A97121901E mnz-10
mantle-1
542 (+/-20)
16.2/0.16
(n=11)
core-2
579 (+/-24)
16.2/0.25
(n=4)
mantle-2
531 (+/-23)
16.8/0.11
(n=6)
core-1
625 (+/-31)
16.5/0.42
(n=5)
rim
538 (+/-26)
16.9/0.30
(n=7)
edge of Bt
COMP — 10μm
XM3175 15.0KV X400

Fig. 9.

REE+P (monazite)=Th+Si (huttonite),
2REE (monazite)=Th+Ca (brabantite).

There is no systematic relationship between monazite age and mode of occurrence; 650–580 Ma monazite domains and grains are present as both inclusions in garnet and in the matrix (Fig. 9). Older (650–550 Ma) cores are occasionally enclosed by 550–500 Ma overgrowths (Fig. 9).

4.3. Monazite ages and chemistry of the Napier Complex sample

Thirteen monazite grains were examined in a thin section of sample 21409, and can be classified into the following modes of occurrence (Fig. 10): (1) 2 grains as inclusions in garnet or sillimanite; (2) one grain as inclusion on an intracrystal fracture in garnet; (3) one grain in biotite-sillimanite aggregate; (4) 4 grains associated with biotite-bearing alteration zones at the edge of garnet porphyroblasts, and (5) 5 grains at grain boundaries of various minerals.

Monazite inclusions in unfractured garnet or sillimanite without any fracturing suggest 2500–2440 Ma ages, consistent with previously reported monazite ages. Monazite associated with biotite-bearing textural domains, biotite-bearing coronas arround garnet, intracrystalline fractures within garnet, or aggregates of fine-grained

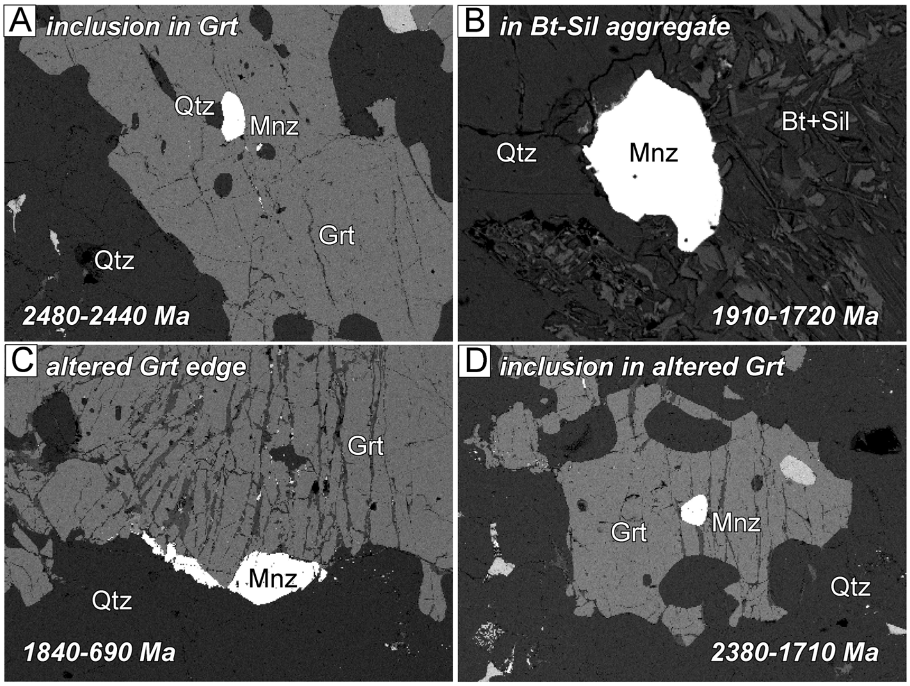

Fig. 10. BEI of monazite grains in garnet-sillimanite gneiss from Mt. Riiser-Larsen. A. Monazite included in garnet porphyroblast. B. Monazite in fine-grained biotite-sillimanite aggregate. C. Monazite grains around altered garnet porphyroblasts. D. Monazite included in garnet with intracrystalline fractures.

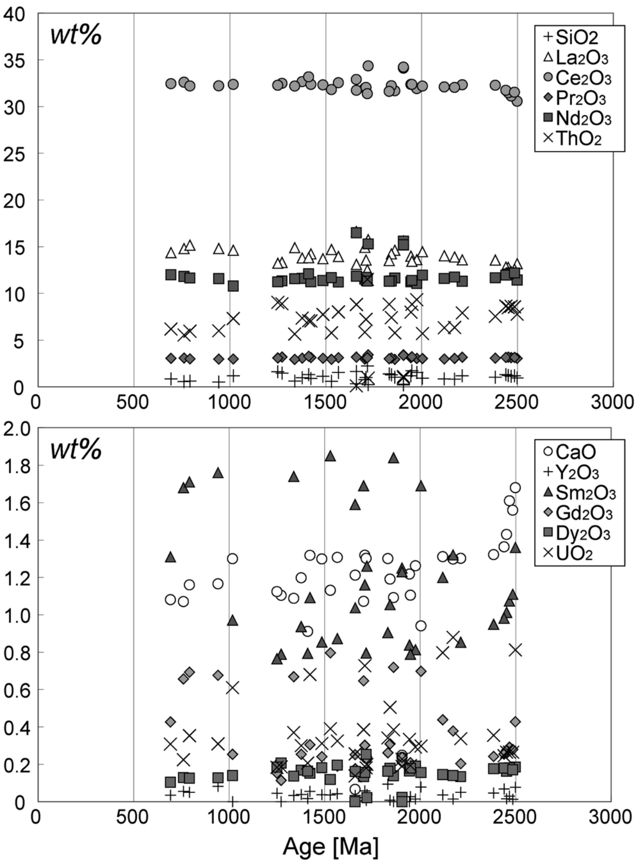

Fig. 11. EMP U-Th-Pb ages versus chemical composition of monazite in metapelite from Mt. Riiser-Larsen area.

biotite-sillimanite yield wider ranging ages from 2400 Ma to 700 Ma. The 2500–2440 Ma monazite has lower La and Ce and higher Ca content than other contexts (Fig. 11). This suggests a change of monazite composition from *c.* 2500 Ma- to younger ages involving substitution of a brabantite component:

$$2\mathrm{REE}\ (\mathrm{monazite}) = \mathrm{Th} + \mathrm{Ca}\ (\mathrm{brabantite}).$$

It is not known what causes this compositional change, which may be controlled by changes in coexisting solid or fluid phases. Younger monazite grains (*e.g.,* grain-#10) in biotite-sillimanite aggregates have distinctively high La, Ce, Nd and Sm (L-MREE) contents and yield 1910–1720 Ma U-Th-Pb chemical ages.

5. Discussion

5.1. Pre- and peak metamorphic processes in the Lützow-Holm Complex

On the basis of SHRIMP U-Pb analyses with detailed CL imaging of zircon grains, Shiraishi *et al.* (2003) demonstrated that amphibolite to granulite-facies metamorphism occurred in the Lützow-Holm Complex at 550–520 Ma. These 550 Ma~ SHRIMP zircon dates are identical with the younger age group (540±5 Ma~554±14 Ma) of our EMP monazite analyses. In contrast, zircon growth at 650–580 Ma, corresponding to older monazite dates, has not been reported (Shiraishi *et al.,* 2003). REE chemical features of 650–580 Ma monazite, such as higher Nd, Sm, Gd and Dy (MREE) contents, indicate changes of the conditions of monazite growth between 650–580 Ma and 550–500 Ma. Such compositional changes may have been controlled by changes in coexisting REE-bearing phases. All of the analyzed samples include garnet, which is one of the major minerals formed in the amphibolite to granulite-facies conditions, and is stable at peak metamorphic temperatures. Relatively M-HREE depleted younger 560–500 Ma monazites were possibly in equilibrium with garnet, which favors M-HREE, whereas MREE-enriched 650–580 Ma monazite may have been stable in garnet-absent assemblages. Some of the < 560 Ma monazite grains included in or surrounded by garnet (*e.g.,* mnz-4 of A97121901B; Fig. 9B) are suggestive of this interpretation. The MREE-enriched > 580 Ma monazites may have been formed as the breakdown of other earlier-stage REE-bearing phases such as apatite or allanite.

Dissolution and crystallization mechanisms of monazite are not fully-understood. Phosphorous and LREE solubility in melt (*e.g.,* Green and Watson, 1982; Rapp and Watson, 1986) is a factor that controls the stability of monazite in partially-molten metamorphic rocks. During the prograde heating to temperatures above the solidus, monazite tends to be dissolved due to phosphorous and LREE solubility in anatectic melt. Monazite can be precipitated from melt during cooling, which causes a decrease in solubility of phosphorous and LREE in melt. Although it is not easy to investigate monazite dissolution-crystallization mechanisms quantitatively, our observation that older 650–580 Ma monazite is absent in the monazite-poor *group-A* samples, but has been preserved widely in the monazite-rich *group-B* samples (Table 5), is consistent with the interpretation, although it is merely hypothetical, that the monazite-poor *group-A* samples have never exceeded the phosphorous and LREE saturation in melt. In contrast, in monazite-rich *group-B* samples, a certain amount of monazite grains have been possibly retained without being completely dissolved in melt, even at the peak of metamorphism, because of excess of phosphorous and LREE over saturation levels in anatectic melt.

According to the above interpretation, the formation of 560–500 Ma monazite is related to peak-T metamorphism. Older 650–580 Ma monazite may have formed in the absence of garnet, and hence pre-dates the formation of garnet under amphibolite to granulite-facies conditions. Fraser (1997) reported the ~620 Ma zircon overgrowth in the garnet-sillimanite-orthopyroxene-bearing pelitic gneiss determined by SHRIMP. It is, however, difficult to determine its exact age and the significance of this event. Similar *c.* 670 Ma ages in the Lützow-Holm Complex have been implied by Sm-Nd whole rock isochron ages interpreted as magmatism (Nishi *et al.,* 2002; Shibata *et al.,* 1986). The formation of 650–580 Ma monazite in our study may be related to such magmatism, although we could not exclude the possibility of these monazite grains being derived from detrital grains in exotic sediments.

It is known that Pan-African events vary widely in age, from 700 to 500 Ma (*e.g.,* Jacobs *et al.,* 2003; Meert, 2003). In the East Antarctic sector, most Pan-African metamorphism occurred in a range of 550–520 Ma (*e.g.,* Shiraishi *et al*., 1994; Asami *et al*., 2005; Boger *et al*., 2002; Jacobs *et al*., 2003; Meert, 2003). It has also been implied that the area including the Lützow-Holm Complex is the conjugate position of two different (700–550 Ma and 550–520 Ma) orogenic belts (Meert, 2003). Further investigation is essential to assess the mutual relationships of pre- and syn- 550–520 Ma events in this area and their regional tectonic implications.

5.2. Peak- and post-peak metamorphism of the Napier Complex

Timing of UHT metamorphism of the Napier Complex has been discussed by many authors (*e.g.,* Harley and Black, 1997; Grew, 1998; Carson *et al*., 2002; Kelly and Harley, 2005), and broadly constrained to an age range of 2590–2480 Ma. Monazite ages presented here are 2480 Ma or younger, and demonstrate monazite growth or re-equilibration after peak UHT metamorphism. The 2480–2440 Ma monazite dates in the sample studied are indicative of crystallization at or during the cooling stage of the UHT metamorphism. Other 2400–700 Ma younger monazites more or less relate with biotite-bearing re-hydration textures. Such hydrous minerals (mostly biotite) are common in the intracrystal fractures of garnet, and we suggest that monazite inclusions in garnet are also affected by isotopic disturbance. Isotopic ages younger than 2400 Ma for the Napier Complex have been reported by several authors (2200 Ma, 1700 Ma and 700 Ma xenotime or monazite ages by Grew *et al*., 2001; 1557 and 1897 Ma Sm-Nd garnet-whole rock ages by Owada *et al*., 2001; 2200 Ma Sm-Nd internal isochron age by Suzuki *et al*., 2001; ~2380 Ma Sm-Nd internal isochron age by Suzuki *et al*., 2006). Our monazite age data presented here, even though scattered, imply the possibility of *c.* 1900–1700 Ma related with biotite-sillimanite grade event; isotopic disturbance also occurred at *c.* 700 Ma.

6. Conclusions

Monazite U-Th-Pb chemical dating with full REE chemical analysis using electron microprobe (EMP) is a potentially powerful tool for obtaining age estimates with chemically contextual information in monazite.

This study reports 650–580 Ma ages, significantly older than 550–520 Ma ages reported by SHRIMP zircon analysis, for the first time from the Lützow-Holm Complex. The younger 560–500 Ma ages apparently relate to metamorphic events in which monazite grew in the presence of garnet, and older 650–580 Ma ages are interpreted on the basis of M-HREE-enriched chemistry to metamorphic growth in garnet-absent assmblages, hence, pre-dating the peak metamorphism in this region.

Monazites from garnet-sillimanite gneiss yield 2500–2440 Ma ages from garnet inclusions and 2400–700 Ma ages from the altered domains. Incomplete monazite chemical disturbance makes it difficult to indicate a certain age event, but, at least, incomplete isotopic resetting at 1900–1700 Ma (biotite-sillimanite-grade ?), and pervasive chemical alteration at 700 Ma, are similar to ages previously reported by Grew *et al.* (2001) and Owada *et al.* (2001).

Acknowledgments

The electron microprobe analytical technique for monazite U-Th-Pb chemical dating was developed with the assistance of Dr. K. Yokoyama at the National Science Museum, Japan. We acknowledge Prof. K. Shiraishi and Dr. D. Dunkley for their valuable comments and discussion for U-Th-Pb dating. Samples used in this study were collected by TH during the 1996–1997 and 1997–1998 Japanese Antarctic Research Expeditions (JARE), and the members of JARE, especially Profs. H. Ishizuka, Y. Osanai, Drs. M. Ishikawa, S. Suzuki, T. Toyoshima, M. Owada, T. Tsunogae and W. A. Crowe are thanked for their support during the field work. Constructive reviews by Prof. K. Suzuki and Dr. D. Dunkley improved the manuscript. This study was financially supported by a Grant-in-Aid for Scientific Research to TH from the Ministry of Education, Culture, Sports, Science and Technology No. 16740298.

References

Asami, M., Suzuki, K. and Adachi, M. (1997): Th, U and Pb analytical data and CHIME dating of monazites from metamorphic rocks of the Rayner, Lützow-Holm, Yamato-Belgica and Sør Rondane Complexes, East Antarctica. Proc. NIPR Symp. Antarct. Geosci., **10**, 130–152.

Asami, M., Suzuki, K., Grew, E.S. and Adachi, M. (1998): CHIME ages for granulites from the Napier Complex, East Antarctica. Polar Geosci., **11**, 172–199.

Asami, M., Suzuki, K. and Grew, E.S. (2002): Chemical Th-U-total Pb dating by electron microprobe analysis of monazite, xenotime and zircon from the Archean Napier Complex, East Antarctica: Evidence for ultra-high-temperature metamorphism at 2400 Ma. Precambrin Res., **114**, 249–275.

Asami, M., Suzuki, K. and Grew, E.S. (2005): Monazite and zircon dating by the chemical Th-U-total Pb isochron method (CHIME) from Alasheyev Blight to the Sør Rondane Mountains, East Antarctica: A reconnaissance study of the Mozambique suture in eastern Queen Maud Land. J. Geol., **113**, 59–82.

Boger, S.D., Carson, C.J., Fanning, C.M., Hergt, J.M., Wilson, C.J.L. and Woodhead, J.D. (2002): Pan-African intraplate deformation in the northern Prince Charles Mountains, east Antarctica. Earth Planet. Sci. Lett., **195**, 195–210.

Carson, C.J., Ague, J.J. and Coath, C.D. (2002): U-Pb geochronology from Tonagh Island, East Antarctica: implications for the timing of ultra-high temperature metamorphism of the Napier Complex. Precambrin Res., **116**, 237–263.

Cocherie, A. and Albarede, F. (2001): An improved U-Th-Pb age calculation for electron microprobe dataing of monazite. Geochim. Cosmochim. Acta, **65**, 4509–4522.

Cocherie, A., Legendre, O., Peucat, J.J. and Kouamelan, A.N. (1998): Geochronology of polygenetic monazites constrained by *in situ* electron microprobe Th-U-total lead determination: Implications for lead behavior in monazite. Geochim. Cosmochim. Acta, **62**, 2475–2497.

Fraser, G.L. (1997): Geochronological constraints on the metamorphic evolution and exhumation of the Lützow-Holm Complex, East Antarctica. Ph.D. Thesis, The Australian National University, 254 p.

Fraser, G.L., McDougall, I., Ellis, D.J. and Williams, I.S. (2000): Timing and rate of isothermal decompression in Pan-African granulites from Rundvågshetta, East Antarctica. J. Metamorph. Geol., **18**, 441–454.

Green, T.H. and Watson, E.B. (1982): Crystallization of apatite in natural magmas under high-pressure hydrous conditions, with particular reference to orogenic rock series. Contrib. Mineral. Petrol., **79**, 96–105.

Grew, E.S. (1998): Boron and beryllium minerals in granulite-facies pegmatites and implications of beryllium pegmatites for the origin and evolution of the Archaean Napier Complex of East Antarctica. Mem. Natl Inst. Polar Res., Spec. Issue, **53**, 74–93.

Grew, E.S., Suzuki, K. and Asami, M. (2001): CHIME ages of xenotime, monazite and zircon from beryllium pegmatites in the Napier Complex, Khmara Bay, Enderby Land, East Antarctica. Polar Geosci., **14**, 99–118.

Harley, S.L. and Black, L.P. (1997): A revised Archaean chronology for the Napier Complex, Enderby Land, from SHRIMP ion-microprobe studies. Antarct. Sci., **9**, 74–91.

Harley, S.L., Kinny, P.D., Snape, I. and Black, L.P. (2001): Zircon chemistry and the definition of events in Archaean granulite terrains. Fourth International Archaean Symposium, Extended abstract, AGSO Geoscience Australia Record 2001/37, 511–513.

Hiroi, Y., Shiraishi, K. and Motoyoshi, Y. (1991): Late Proterozoic paired metamorphic complexes in East Antarctica, with special reference to the tectonic significance of ultramafic rocks. Geological Evolution of Antarctica, ed. by M.R.A. Thomson *et al.* Cambridge, Cambridge Univ. Press, 83–87.

Hokada, T., Misawa, K., Shiraishi, K. and Suzuki, S. (2003): Mid to Late Archaean (3.3–2.5 Ga) tonalitic crustal formation and high-grade metamorphism at Mt. Riiser-Larsen, Napier Complex, East Antarctica. Precambrin Res., **127**, 215–228.

Hokada T., Misawa K., Yokoyama K., Shiraishi K. and Yamaguchi A. (2004): SHRIMP and electron microprobe chronology of UHT metamorphism in the Napier Complex, East Antarctica: implications for zircon growth at >1000°C. Contrib. Mineral. Petrol, **147**, 1–20.

Holmes, A. (1931): Radioactivity and geological time. Physics of the Earth—IV The Age of the Earth, ed. by A. Knopf. Washington D.C., The National Research Council of the National Academy of Sciences, 124–459 (Bull. Natl Res. Counc. (U.S.)).

Ishikawa, M., Hokada, T., Ishizuka, H., Miura, H., Suzuki, S. and Takada, M. (2000): Geological map of Mt. Riiser-Larsen, Enderby Land, Antarctica. Antarct. Geol. Map Ser., Sheet 37 (with explanatory text 23 p.). Tokyo, Natl. Inst. Polar Res.

Ishizuka, H., Ishikawa, M., Hokada, T. and Suzuki, S. (1998): Geology of the Mt. Riiser-Larsen area of the Napier Complex, Enderby Land, East Antarctica. Polar Geosci., **11**, 154–171.

Jacobs, J., Bauer, W. and Fanning, C.M. (2003): Late Neoproterozoic/early Palaeozoic events in central Dronning Maud Land and significance for the southern extension of the East African Orogen into East Antarctica. Precambrin Res., **126**, 27–53.

Jercinovic, M.J. and Williams, M.L. (2005): Analytical perils (and progress) in electron microprobe trace element analysis applied to geochronology: background acquisition, interferences, and beam irradiation effects. Am. Mineral., **90**, 526–546

Kelly, N.M. and Harley, S.L. (2005): An integrated microtextural and chemical approach to zircon geochronology: refining the Archaean history of the Napier Complex, east Antarctica. Contrib. Mineral. Petrol., **149**, 57–84.

Kiyokawa, S., Byrne, T., Taira, A., Sano, Y. and Bowring, S. (2002): Structural evolution of the middle Archean, coastal Pilbara terrane, Western Australia. Tectonics, DOI 10.1029/2001TC001296.

Kretz, R. (1983): Symbols for rock-forming minerals. Am. Mineral., **68**, 277–279.

Knoper, M., Armstrong, R.A., Andreoli, M.A.G. and Ashwal, L.D. (2001): The Steenkampskraal monazite vein: a subhorizontal stretching shear zone indicating extensional collapse of Namaqualand at 1033 Ma? J. Afr. Earth Sci., **30** (Suppl.), 38–39.

Ludwig, K.R. (2001): Iwoplot/Ex rev. 2.49: a geochronological tool kit for Microsoft Excel. Berkeley Geochronology Center Special Publication No. 1a, 55 p.

Meert, J.G. (2003): A synopsis of events related to the assembly of eastern Gondwana. Tectonophysics, **362**, 1–40.

Montel, J.M., Foret, S., Veschambre, M., Nicollet, C. and Provost, A. (1996): Electron microprobe dating of monazite. Chem. Geol., **131**, 37–53.

Motoyoshi, Y. and Ishikawa, M. (1997): Metamorphic and structural evolution of granulites from Rundvågshetta, Lützow-Holm Bay, East Antarctica. The Antarctic Region: Geological Evolution and Processes, ed. by C.A. Ricci. Siena, Terra Antarct. Publ., 65–72.

Nishi, N., Kawano, Y. and Kagami, H. (2002): Rb-Sr and Sm-Nd isotopic geochronology of the granitoid and hornblende biotite gneiss from Oku-iwa Rock in the Lützow-Holm Complex, East Antarctica. Polar Geosci., **15**, 46–65.

Osanai, Y., Toyoshima, T., Owada, M., Tsunogae, T., Hokada, T., Crowe, W.A., Ikeda, T., Kawakami, T., Kawano, Y., Kawasaki, T., Ishikawa, M., Motoyoshi, Y. and Shiraishi, K. (2004): Geological map of Skallen, Antarctica (Revised Edition). Antarct. Geol. Map Ser., Sheet 39 (with explanatory text 23 p.). Tokyo, Natl. Inst. Polar Res.

Owada, M., Osanai, Y., Tsunogae, T., Hamamoto, T., Kagami, H., Toyoshima, T. and Hokada, T. (2001): Sm-Nd garnet ages of retrograde garnet bearing granulites from Tonagh Island in the Napier Complex, East Antarctica: a preliminary study. Polar Geosci., **14**, 75–87.

Pyle, J.M., Spear, F.S., and Wark, D.A. (2002): Electron microprobe analysis of REE in apatite, monazite, and xenotime: protocols and pitfalls. Phosphates: Geochemical, Geobiological, and Materials Importance, ed. by M.J. Kohn *et al.* Washington, D.C., Mineralogical Society of America, 337–362 (Rev. Mineral. Geochem. Ser. 48).

Pyle, J.M., Spear, F.S., Wark, D.A., Daniel, C.G. and Storm, L.C. (2005): Contribution to precision and accuracy of chemical ages of monazite. Am. Mineral., **90**, 547–577.

Rapp, R.P. and Watson, E.B. (1986): Monazite solubility and dissolution kinetics: implications for the thorium and light rare earth chemistry of felsic magmas. Contrib. Mineral. Petrol., **94**, 309–316.

Sano, Y., Tsutsumi, Y., Terada, K. and Kaneoka, I. (2003): Ion microprobe U-Pb dating of Quaternary zircon: implications for magma cooling and residence time. J. Volcanol. Geotherm. Res., **117**, 285–296.

Scherrer, N.C., Engi, M., Gnos, E., Jokob, V. and Liechti, A. (2000): Monazite analysis; from sample preparation to microprobe age dating and REE quantification, Schweiz. Mineral. Petrogr. Mitt., **80**, 93–105.

Sheraton, J.W., Tingey, R.J., Black, L.P., Offe, L.A. and Ellis, D.J. (1987): Geology of Enderby Land and western Kemp Land, Antarctica. BMR Bull., **223**, 51 p. (with geological map).

Shibata, K., Yanai, K. and Shiraishi, K. (1986): Rb-Sr whole-rock ages of metamorphic rocks from eastern Queen Maud Land, East Antarctica. Mem. Natl Inst. Polar Res., Spec. Issue, **43**, 133–148.

Shiraishi, K., Ellis, D.J., Hiroi, Y., Fanning, C.M., Motoyoshi, Y. and Nakai, Y. (1994): Cambrian orogenic belt in East Antarctica and Sri Lanka: Implications for Gondwana Assembly. J. Geol., **102**, 47–65.

Shiraishi, K., Hokada, T., Fanning, C.M., Misawa, K. and Motoyoshi, Y. (2003): Timing of thermal events in eastern Dronning Maud Land, East Antarctica. Polar Geosci., **16**, 76–99.

Steiger, R.H. and Jäger, E. (1977): Subcommision on geochronology: convention on the use of decay constants in geo- and cosmochronology. Earth Planet. Sci. Lett., **36**, 359–362.

Suzuki, K. (2005): CHIME (Chemical Th-U-total Pb isochron method) dating on the basis of electron microprobe analysis. J. Geol. Soc. Jpn., **111**, 509–526 (in Japanese with English abstract).

Suzuki, K. and Adachi, M. (1991): Precambrian provenance and Silurian metamorphism of the Tsubonosawa paragneiss in South Kitakami terrane, revealed by the chemical Th-U-total Pb isochron ages of monazite, zircon and xenotime. Geochem. J., **25**, 357–376.

Suzuki, K., Adachi, M. and Tanaka, T. (1991): Middle Precambrian provenance of Jurassic sandstone in the Mino Terrane, central Japan: Th-U-total Pb evidence from an electron microprobe monazite study. Sediment. Geol., **75**, 141–147.

Suzuki, S., Kagami, H., Ishizuka, H. and Hokada, T. (2001): Sm-Nd mineral isochron age of sapphirine-quartz gneiss from the Mt. Riiser-Larsen area in the Napier Complex, East Antarctica. Polar Geosci., **14**, 88–98.

Suzuki, S., Arima, M., Williams, I.S., Shiraishi, K. and Kagami, H. (2006): Thermal history of UHT metamorphism in the Napier Complex, East Antarctica: Insights from zircon, monazite and garnet ages. J. Geol., **114**, 65–84.

Williams, M.L. and Jercinovic, M.J. (2002): Microprobe monazite geochronology: putting absolute time into microstructural analysis. J. Struct. Geol., **24**, 1013–1028.

Williams, M.L., Jercinovic, M.J. and Terry, M.P. (1999): Age mapping and dating of monazite on the electron microprobe: deconvoluting multi-stage histories. Geology, **27**, 1023–1026.

Yokoyama, K. and Saito, Y. (1996): Petrological study of pre-Tertiary sandstones in the South Kitakami Massif, Northeast Japan. Mem. Natl Sci. Mus., **29**, 9–24.

Zhu, X.K. and O'Nions, R.K. (1999): Monazite chemical composition: some implications for monazite geochronology. Contrib. Mineral. Petrol., **137**, 351–363.

Appendix
Theoretical basis and error propagation of U-Th-Pb age determination

A detailed explanation of U-Th-Pb age calculation is given in Suzuki (2005) and references therein, and is briefly summarized in this appendix. Long-lived isotopes of uranium and thorium decay to isotopes of Pb with half lives of 4470 million years (^{238}U), 704 million years (^{235}U) and 1.4 billion years (^{232}Th) as follows (n = numbers of isotope, t = year, and λ = decay constant after Steiger and Jäger, 1977):

$$n_{^{206}\mathrm{Pb}} = n_{^{238}\mathrm{U}}\{\exp(\lambda_{238}\,t) - 1\}, \qquad \lambda_{238} = 1.55125 \times 10^{-10}$$
$$n_{^{207}\mathrm{Pb}} = n_{^{235}\mathrm{U}}\{\exp(\lambda_{235}\,t) - 1\}, \qquad \lambda_{235} = 9.8485 \times 10^{-10}$$
$$n_{^{208}\mathrm{Pb}} = n_{^{232}\mathrm{Th}}\{\exp(\lambda_{232}\,t) - 1\}. \qquad \lambda_{232} = 4.9475 \times 10^{-11}$$

An electron microprobe allows not isotopic analysis but chemical analysis, and the measured total of U, Th and Pb oxide weight percentages can be converted to the sum of the numbers of isotopes as follows (w = oxide wt% and M = molecular weight):

$$n_{^{235}\mathrm{U}} + n_{^{238}\mathrm{U}} = \text{total}\, n_{\mathrm{U}} = \frac{w_{\mathrm{UO_2}}}{M_{\mathrm{UO_2}}},$$

$$n_{^{232}\mathrm{Th}} = \text{total}\, n_{\mathrm{Th}} = \frac{w_{\mathrm{ThO_2}}}{M_{\mathrm{ThO_2}}},$$

$$n_{^{208}\mathrm{Pb}} + n_{^{207}\mathrm{Pb}} + n_{^{206}\mathrm{Pb}} = \text{total}\, n_{\mathrm{Pb}} = \frac{w_{\mathrm{PbO}}}{M_{\mathrm{PbO}}}.$$

Assuming no isotopic fractionation of uranium (^{238}U/^{235}U = 137.88: present value after Steiger and Jäger, 1977), age (t) can be calculated using the following equation:

$$\text{Total}\, n_{\mathrm{Pb}} = n_{\mathrm{Pb,initial}} + n_{\mathrm{Th}}\left\{\exp(\lambda_{232}t) - 1\right\} + n_{\mathrm{U}}\left\{\frac{\exp(\lambda_{235}t) + 137.88\exp(\lambda_{238}t)}{138.88} - 1\right\}.$$

The initial Pb is normally below the detection limit of electron microprobe analysis, and the above equation can be re-written as:

$$\frac{w_{\mathrm{PbO}}}{M_{\mathrm{PbO}}} = \frac{w_{\mathrm{ThO_2}}}{M_{\mathrm{ThO_2}}}\left\{\exp(\lambda_{232}t) - 1\right\} + \frac{w_{\mathrm{UO_2}}}{M_{\mathrm{UO_2}}}\left\{\frac{\exp(\lambda_{235}t) + 137.88\exp(\lambda_{238}t)}{138.88} - 1\right\}.$$

Error propagation of U-Th-Pb age is based on X-ray counting statistics of electron microprobe analysis. The following three different methods have been applied in this study (w (s.d.) = standard deviation based on X-ray counting statistics):

A1. Error propagation simply by the root mean square of U, Th, Pb X-ray counting errors (%)

$$\text{Age-error-1(Ma)} = t(\text{Ma}) \times \frac{\text{Age-error-1(\%)}}{100},$$

where Age-error-1 (%) can be calculated by the following equation:

$$\text{Age-error-1}(\%)=\sqrt{(\text{error-U}(\%))^2+(\text{error-Th}(\%))^2+(\text{error-Pb}(\%))^2},$$

$$\text{error-U}(\%)=\frac{w(\text{s.d.})_{UO_2}}{w_{UO_2}}\times 100,$$

$$\text{error-Th}(\%)=\frac{w(\text{s.d.})_{ThO_2}}{w_{ThO_2}}\times 100,$$

$$\text{error-Pb}(\%)=\frac{w(\text{s.d.})_{PbO}}{w_{PbO}}\times 100.$$

A2. Error propagation by the root mean square of U, Th and Pb contributions to age errors (Ma) converted by the X-ray counting errors (%)

$$\text{Age-error-2}(\text{Ma})=\sqrt{(\text{error-U}(\text{Ma}))^2+(\text{error-Th}(\text{Ma}))^2+(\text{error-Pb}(\text{Ma}))^2},$$

where error-U, error-Th and error-Pb can be estimated by solving the following equations:

$$\frac{w_{PbO}}{M_{PbO}}=\frac{w_{ThO_2}}{M_{ThO_2}}\left\{\exp(\lambda_{232}\,\text{error-U}(\text{Ma}))-1\right\}+\frac{w(\text{s.d.})_{UO_2}}{M_{UO_2}}\left\{\frac{\exp(\lambda_{235}\,\text{error-U}(\text{Ma}))+137.88\exp(\lambda_{238}\,\text{error-U}(\text{Ma}))}{138.88}-1\right\},$$

$$\frac{w_{PbO}}{M_{PbO}}=\frac{w(\text{s.d.})_{ThO_2}}{M_{ThO_2}}\left\{\exp(\lambda_{232}\,\text{error-Th}(\text{Ma}))-1\right\}+\frac{w_{UO_2}}{M_{UO_2}}\left\{\frac{\exp(\lambda_{235}\,\text{error-Th}(\text{Ma}))+137.88\exp(\lambda_{238}\,\text{error-Th}(\text{Ma}))}{138.88}-1\right\},$$

$$\frac{w(\text{s.d.})_{PbO}}{M_{PbO}}=\frac{w_{ThO_2}}{M_{ThO_2}}\left\{\exp(\lambda_{232}\,\text{error-Pb}(\text{Ma}))-1\right\}+\frac{w_{UO_2}}{M_{UO_2}}\left\{\frac{\exp(\lambda_{235}\,\text{error-Pb}(\text{Ma}))+137.88\exp(\lambda_{238}\,\text{error-Pb}(\text{Ma}))}{138.88}-1\right\}.$$

A3. Error propagation by the root mean square of U, Th and Pb contributions to age errors (Ma) converted by the X-ray counting errors (%) based on the simplified age (T) calculation equation

Age-error-3 is similar with age-error-2, but is based on the rather simple age calculation equation proposed by Holmes (1931) as follows:

$$T(\mathrm{Ma})=\frac{n_{\mathrm{Pb}}}{n_{\mathrm{U}}+0.36\,n_{\mathrm{Th}}}\times 7600.$$

Based on the above equation, age error propagation is calculated by differentiating partially with respect to U, Th and Pb as follows:

$$\text{Age-error-3}(\mathrm{Ma})=\sqrt{(\text{error-U}(\mathrm{Ma}))^2+(\text{error-Th}(\mathrm{Ma}))^2+(\text{error-Pb}(\mathrm{Ma}))^2}$$

$$=\sqrt{\left(\frac{\partial T}{\partial w_{\mathrm{UO_2}}}w(\mathrm{s.d.})_{\mathrm{UO_2}}\right)^2+\left(\frac{\partial T}{\partial w_{\mathrm{ThO_2}}}w(\mathrm{s.d.})_{\mathrm{ThO_2}}\right)^2+\left(\frac{\partial T}{\partial w_{\mathrm{PbO}}}w(\mathrm{s.d.})_{\mathrm{PbO}}\right)^2}$$

$$=\Bigg[\left\{-\left(\frac{w_{\mathrm{PbO}}}{M_{\mathrm{PbO}}}\right)/\left(\frac{w_{\mathrm{UO_2}}}{M_{\mathrm{UO_2}}}+0.36\times\frac{w_{\mathrm{ThO_2}}}{M_{\mathrm{ThO_2}}}\right)^2\right\}$$

$$+\left\{-\left(\frac{w_{\mathrm{PbO}}}{M_{\mathrm{PbO}}}/0.36\right)/\left(\frac{w_{\mathrm{UO_2}}}{M_{\mathrm{UO_2}}}/0.36+\frac{w_{\mathrm{ThO_2}}}{M_{\mathrm{ThO_2}}}\right)^2\right\}$$

$$+\left\{1/\left(\frac{w_{\mathrm{UO_2}}}{M_{\mathrm{UO_2}}}+0.36\times\frac{w_{\mathrm{ThO_2}}}{M_{\mathrm{ThO_2}}}\right)^2\right\}\Bigg]^{1/2}.$$

Appendix-1. Comparison of three different calculations of error propagation based on X-ray counting statistics. 'Age-error-1' commonly overestimates the contribution of U onto the error propagation (error-U) due to relatively lower UO_2 than ThO_2 in monazite. 'Age-error-2' and 'Age-error-3' yield similar values with each other, and the 'error-3' is used in this study. See 'Appendix' for detail.

		Namaqualand monazite			Napier monazite		
spot		#-1	#-2	#-3	#-1	#-2	#-3
UO_2	(wt%)	0.218	0.205	0.221	0.413	0.424	0.365
ThO_2	(wt%)	8.110	8.110	8.240	10.070	9.940	4.250
PbO	(wt%)	0.393	0.395	0.398	1.282	1.282	0.612
ThO_2*	(wt%)	8.863	8.819	9.002	11.740	11.656	5.715
Age (t)	(Ma)	**1033**	**1043**	**1030**	**2455**	**2471**	**2413**
Age-error-1	(Ma)	**38**	**40**	**37**	**44**	**43**	**55**
error	*(%)*	*3.7*	*3.9*	*3.6*	*1.8*	*1.7*	*2.3*
error-U	(Ma)	33	36	33	42	41	46
error-Th	(Ma)	2	2	2	4	4	10
error-Pb	(Ma)	18	18	18	13	13	28
Age-error-2	(Ma)	**18**	**18**	**18**	**14**	**14**	**29**
error-U	(Ma)	3	3	3	6	6	11
error-Th	(Ma)	2	2	2	4	4	7
error-Pb	(Ma)	18	18	18	13	13	26
Age-error-3	(Ma)	**21**	**21**	**20**	**17**	**18**	**37**
error-U	(Ma)	3	3	3	5	5	11
error-Th	(Ma)	2	2	2	5	5	10
error-Pb	(Ma)	20	21	20	16	16	34
Age (T)	*(Ma)*	*1150*	*1161*	*1146*	*2913*	*2940*	*2962*

Age (T): age calculation by the relatively simple equation proposed by Holmes (1931)

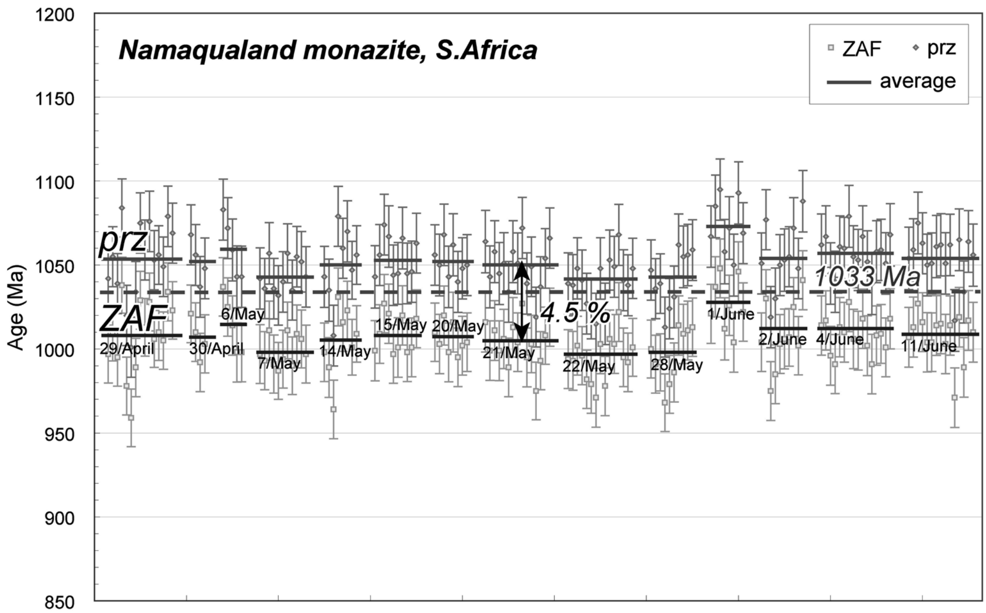

Appendix-2. Comparison of the different matrix correction methods of electron micropobe analysis, and their longterm drift. ZAF correction gives consistently 4.5% younger ages than prz correction.

Appendix-3. Average and standard deviation of representative electron microprobe analysis of Namaqualand monazite, and comparison between prz and ZAF corrections.

Sample	Namaqualand monazite												Namaqualand monazite*			
Matrix cor.	prz		prz		prz		prz		prz		prz		prz*		ZAF*	
Date	2004-6-19		2004-6-25		2004-06-26		2004-07-02		2004-07-09		2004-07-23		2004-06-11		2004-06-11	
	average	*s.d.*	*average*	*s.d.*	*average*	*s.d.*	*average*	*s.d.*	*average*	*s.d.*	*average*	*s.d.*	*average*	*s.d.*	*average*	*s.d.*
Wt%	*n=31*		*n=12*		*n=16*		*n=20*		*n=18*		*n=16*		*n=15*		*n=15*	
P_2O_5	29.03	*0.61*	28.16	*0.50*	27.91	*0.62*	31.32	*0.59*	28.42	*1.42*	26.88	*0.76*	29.43	*0.54*	30.27	*0.58*
SiO_2	1.02	*0.09*	0.94	*0.06*	1.02	*0.06*	1.09	*0.07*	1.00	*0.04*	1.15	*0.07*	1.12	*0.08*	1.05	*0.07*
CaO	1.12	*0.10*	1.14	*0.08*	1.07	*0.06*	1.11	*0.06*	1.10	*0.09*	1.15	*0.07*	1.11	*0.08*	1.16	*0.08*
Y_2O_3	2.34	*0.05*	2.24	*0.05*	2.24	*0.14*	2.42	*0.06*	2.27	*0.08*	2.66	*0.09*	2.52	*0.05*	2.42	*0.04*
La_2O_3	13.02	*0.11*	12.93	*0.11*	13.09	*0.15*	12.95	*0.17*	12.91	*0.17*	12.89	*0.16*	12.93	*0.10*	13.15	*0.10*
Ce_2O_3	27.33	*0.28*	27.33	*0.18*	27.43	*0.36*	27.46	*0.21*	26.62	*0.33*	26.73	*0.19*	27.27	*0.21*	27.73	*0.21*
Pr_2O_3	3.44	*0.12*	3.44	*0.07*	3.44	*0.06*	3.49	*0.09*	3.35	*0.08*	3.40	*0.08*	3.49	*0.07*	3.64	*0.07*
Nd_2O_3	11.09	*0.15*	11.08	*0.08*	11.06	*0.10*	11.10	*0.13*	10.87	*0.13*	10.98	*0.10*	10.89	*0.15*	11.02	*0.15*
Sm_2O_3	1.74	*0.07*	1.76	*0.07*	1.71	*0.06*	1.76	*0.08*	1.68	*0.07*	1.67	*0.07*	1.79	*0.06*	1.89	*0.07*
Gd_2O_3	1.21	*0.14*	1.20	*0.10*	1.21	*0.09*	1.20	*0.09*	1.19	*0.11*	1.19	*0.13*	1.17	*0.11*	1.22	*0.11*
Dy_2O_3	0.62	*0.04*	0.64	*0.04*	0.63	*0.04*	0.63	*0.04*	0.61	*0.05*	0.62	*0.04*	0.63	*0.06*	0.65	*0.06*
Er_2O_3	0.16	*0.04*	0.16	*0.04*	0.16	*0.03*	0.15	*0.03*	0.18	*0.03*	0.19	*0.03*	0.16	*0.03*	0.16	*0.03*
Yb_2O_3	0.06	*0.04*	0.05	*0.04*	0.07	*0.04*	0.06	*0.03*	0.06	*0.03*	0.07	*0.03*	0.05	*0.04*	0.05	*0.04*
UO_2	0.21	*0.01*	0.20	*0.01*	0.21	*0.01*	0.20	*0.01*	0.20	*0.01*	0.15	*0.02*	0.22	*0.01*	0.23	*0.01*
ThO_2	8.41	*0.10*	8.26	*0.05*	8.29	*0.14*	8.35	*0.07*	8.30	*0.10*	8.57	*0.11*	8.31	*0.09*	8.66	*0.09*
PbO	0.40	*0.01*	0.40	*0.00*	0.40	*0.01*	0.40	*0.01*	0.40	*0.01*	0.40	*0.01*	0.41	*0.01*	0.41	*0.01*
Total	101.69	*0.83*	100.45	*0.55*	100.42	*0.82*	104.19	*0.81*	99.64	*1.39*	99.25	*0.85*	102.02	*0.71*	104.24	*0.76*
Cations (O=4)																
P	0.956	*0.008*	0.947	*0.007*	0.942	*0.009*	0.983	*0.006*	0.955	*0.019*	0.925	*0.011*	0.960	*0.007*	0.965	*0.007*
Si	0.040	*0.003*	0.037	*0.003*	0.041	*0.002*	0.040	*0.003*	0.040	*0.002*	0.047	*0.003*	0.043	*0.003*	0.040	*0.003*
Ca	0.047	*0.004*	0.049	*0.003*	0.046	*0.003*	0.044	*0.002*	0.047	*0.003*	0.050	*0.003*	0.046	*0.003*	0.047	*0.004*
Y	0.048	*0.001*	0.047	*0.001*	0.047	*0.003*	0.048	*0.001*	0.048	*0.001*	0.058	*0.002*	0.052	*0.001*	0.049	*0.001*
La	0.187	*0.003*	0.189	*0.003*	0.192	*0.003*	0.177	*0.003*	0.189	*0.006*	0.193	*0.003*	0.184	*0.003*	0.183	*0.003*
Ce	0.389	*0.006*	0.398	*0.004*	0.400	*0.006*	0.373	*0.005*	0.387	*0.013*	0.398	*0.007*	0.385	*0.005*	0.382	*0.005*
Pr	0.049	*0.002*	0.050	*0.001*	0.050	*0.001*	0.047	*0.001*	0.049	*0.002*	0.050	*0.001*	0.049	*0.001*	0.050	*0.001*
Nd	0.154	*0.002*	0.157	*0.002*	0.158	*0.003*	0.147	*0.003*	0.154	*0.004*	0.159	*0.004*	0.150	*0.003*	0.148	*0.003*
Sm	0.023	*0.001*	0.024	*0.001*	0.024	*0.001*	0.022	*0.001*	0.023	*0.001*	0.023	*0.001*	0.024	*0.001*	0.025	*0.001*
Gd	0.016	*0.002*	0.016	*0.001*	0.016	*0.001*	0.015	*0.001*	0.016	*0.002*	0.016	*0.002*	0.015	*0.001*	0.015	*0.001*
Dy	0.008	*0.001*	0.008	*0.001*	0.008	*0.001*	0.007	*0.000*	0.008	*0.001*	0.008	*0.000*	0.008	*0.001*	0.008	*0.001*
Er	0.002	*0.000*	0.002	*0.001*	0.002	*0.000*	0.002	*0.000*	0.002	*0.000*	0.002	*0.000*	0.002	*0.000*	0.002	*0.000*
Yb	0.001	*0.000*	0.001	*0.000*	0.001	*0.000*	0.001	*0.000*	0.001	*0.000*	0.001	*0.000*	0.001	*0.001*	0.001	*0.001*
U	0.002	*0.000*	0.002	*0.000*	0.002	*0.000*	0.002	*0.000*	0.002	*0.000*	0.001	*0.000*	0.002	*0.000*	0.002	*0.000*
Th	0.074	*0.002*	0.075	*0.001*	0.075	*0.002*	0.070	*0.001*	0.075	*0.003*	0.079	*0.002*	0.073	*0.001*	0.074	*0.001*
Pb	0.004	*0.000*	0.004	*0.000*	0.004	*0.000*	0.004	*0.000*	0.004	*0.000*	0.004	*0.000*	0.004	*0.000*	0.004	*0.000*
Total	2.007	*0.004*	2.014	*0.005*	2.015	*0.005*	1.989	*0.004*	2.007	*0.011*	2.024	*0.007*	2.003	*0.004*	2.001	*0.005*
Nd/La	0.444	*0.007*	0.447	*0.006*	0.441	*0.004*	0.447	*0.009*	0.439	*0.008*	0.44	*0.01*	0.44	*0.01*	0.44	*0.01*
Gd/Nd	0.254	*0.029*	0.253	*0.021*	0.254	*0.020*	0.252	*0.018*	0.255	*0.025*	0.25	*0.03*	0.25	*0.02*	0.26	*0.02*
ThO_2*	9.139	*0.110*	8.966	*0.062*	9.005	*0.172*	9.039	*0.098*	9.004	*0.122*	9.07	*0.15*	9.07	*0.11*	9.46	*0.11*
Th/U	40.514	*1.687*	41.274	*1.737*	40.696	*1.579*	42.954	*1.955*	41.827	*2.558*	61.55	*10.28*	38.86	*2.20*	38.39	*2.16*
Age [Ma]	1025	*14*	1033	*16*	1028	*11*	1034	*14*	1030	*23*	1025	*14*	1053	*23*	1008	*22*
+/- [Ma]	20		21		20		20		20		20		20		19	

* Electron microprobe analytical data using the previous analytical setting (different background positioning and interference corrections). The chemical data based on the two different matrix corrections (prz and ZAF) are re-calculated by off-line calibration using the same dataset.